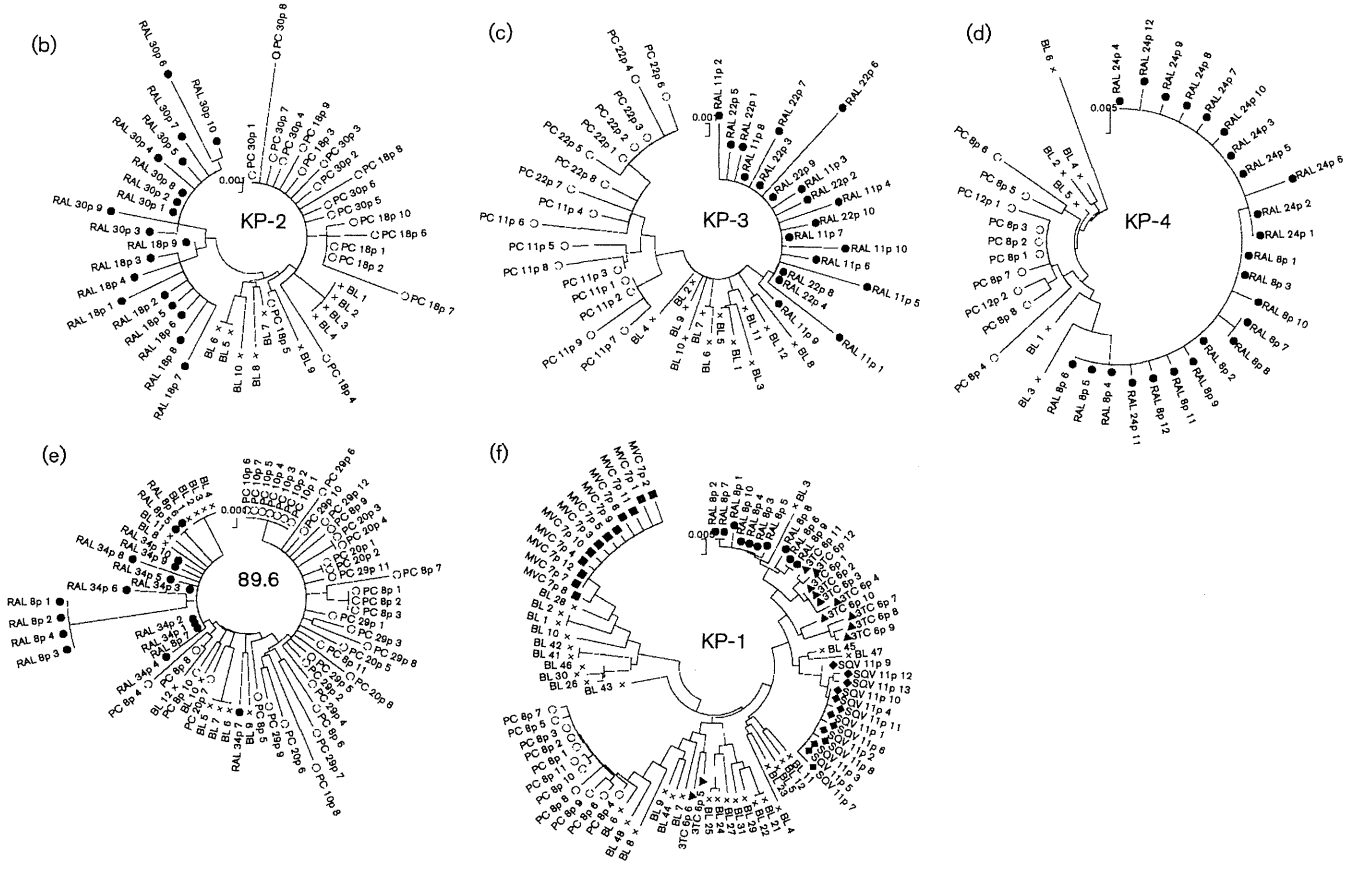

first CCR5 inhibitor (Gulick *et al.*, 2008). One important advantage associated with this drug is the absence of cross-resistance with previously available ARV compounds (Gulick *et al.*, 2008; Steigbigel *et al.*, 2008). However, as is usual with anti-HIV drugs, resistant variants with mutations in the Env, gp120 and gp41 sequences are induced both *in vivo* and *in vitro* (Anastassopoulou *et al.*, 2009; Berro *et al.*, 2009; Tilton *et al.*, 2010; Yoshimura *et al.*, 2009, 2010a). As shown in the present study, distinct Env sequences from each quasispecies might be selected by the different anti-HIV drugs (e.g. length of the V1/2 and/or V4 regions, V3 region depletion and the number of PNGs). Moreover, many of the novel anti-retroviral drugs in pre-clinical trials are viral entry inhibitors (e.g. PRO140, ibalizumab, BMS-663068 and PF-232798; Jacobson *et al.*, 2010; McNicholas *et al.*, 2010; Nettles *et al.*, 2011; Stupple *et al.*, 2011; Toma *et al.*, 2011). Therefore, it is necessary to examine whether such entry inhibitors are effective when used alongside conventional drugs.

In conclusion, we studied the genetic bottleneck in bulk primary HIV-1 isolates from untreated patients and drugs targeting the Env (and other) regions. The results showed, for the first time, the presence of drug-selected Env sequences in these isolates. Although our observations were based on a limited number of HIV-1 isolates and need to be confirmed by independent studies, we believe that they provide a new paradigm for HIV-1 evolution in the new combination ARV therapy era.

METHODS

Patients and isolates. Primary HIV-1 isolates were isolated from four drug-naïve patients in our laboratory (KP-1–4) and passaged in phytohaemagglutinin-activated PBMCs. Infected PBMCs were then co-cultured for 5 days with PM1/CCR5 cells (a kind gift from Dr Y. Maeda; Maeda *et al.*, 2008; Yusa *et al.*, 2005) and the culture supernatants were stored at −150 °C (Hatada *et al.*, 2010; Shibata *et al.*, 2007; Yoshimura *et al.*, 2006, 2010b).

After isolation of the primary viruses, we checked the sensitivity of each primary isolate to MVC. The KP-1 isolate was relatively MVC-resistant compared with KP-2 and KP-3 (54 vs 5.9 and 8.7 nM, respectively). KP-1 became MVC sensitive after eight passages in PM1/CCR5 cells [IC_{50}, 3.4 nM; Geno2pheno value (see below), 41.2 %], whilst under the pressure of MVC, KP-1 became highly resistant to MVC after eight passages (IC_{50}, >1000 nM; Geno2pheno value, 1.7 %). These results indicated that the bulk KP-1 isolate used in this study harboured primarily R5 viruses with X4- or dual-tropic viruses as a minor population.

Cells, culture conditions and reagents. PM1/CCR5 cells were maintained in RPMI 1640 (Sigma) supplemented with 10 % heat-inactivated FCS (HyClone Laboratories), 50 U penicillin ml^{-1}, 50 μg streptomycin ml^{-1} and 0.1 mg G418 (Nacalai Tesque) ml^{-1}. MVC, RAL and SQV were kindly provided by Pfizer, Merck & Co. and Roche Products, respectively. 3TC was purchased from Wako Pure Chemical Industries.

The laboratory-adapted HIV-1 strain 89.6, which was obtained through the NIH AIDS Research and Reference Reagent Program, was propagated in phytohaemagglutinin-activated PBMCs. The viral-competent library pJR-FL-V3Lib, which contains 176 bp V3–loop DNA fragments with 0–10 random combinations of amino acid substitutions, was introduced into pJR-FL, as described previously (Yusa *et al.*, 2005).

***In vitro* selection of HIV-1 variants using anti-HIV drugs.** The four primary HIV isolates (KP-1–4), strain 89.6 and JR-FL-V3Lib were treated with various concentrations of RAL and used to infect PM1/CCR5 cells to induce the production of RAL-selected HIV-1 variants, as described previously, with minor modifications (Hatada *et al.*, 2010; Shibata *et al.*, 2007; Yoshimura *et al.*, 2006, 2010b). Briefly, PM1/CCR5 cells (4×10^4 cells) were exposed to 500 $TCID_{50}$ HIV-1 isolates and cultured in the presence of RAL. Virus replication in PM1/CCR5 cells was monitored by observing the cytopathic effects. The culture supernatant was harvested on day 7 and used to infect fresh PM1/CCR5 cells for the next round of culture in the presence of increasing concentrations of RAL. When the virus began to propagate in the presence of the drug, the compound concentration was increased further. Proviral DNA was extracted from lysates of infected cells at different passages using a QIAamp DNA Blood Mini kit (Qiagen). The proviral DNAs obtained were then subjected to nucleotide sequencing. *In vitro* selection of the KP-1 isolate using SQV, 3TC and MVC was also performed using the procedure described above.

Amplification of proviral DNA and nucleotide sequencing. Proviral DNA was subjected to PCR amplification using PrimeSTAR GXL DNA polymerase and Ex-*Taq* polymerase (Takara), as described previously (Hatada *et al.*, 2010; Shibata *et al.*, 2007; Yoshimura *et al.*, 2006, 2010b). The primers used were 1B and H for the gp120 region (Hatada *et al.*, 2010; Shibata *et al.*, 2007; Yoshimura *et al.*, 2006, 2010b), IN 1F (5′-CAGACTCACAATATGCATTAGG-3′) and IN 1R (5′-CCTGTATGCAGACCCCAATATG-3′) for the *IN* region, and IN 1F and H for the *IN*–gp120 region. The first-round PCR products were used directly in a second round of PCR using primers 2B and F (Hatada *et al.*, 2010; Shibata *et al.*, 2007; Yoshimura *et al.*, 2006, 2010b) for gp120, IN 2F (5′-CTGGCATGGGTACCAGCACACAA-3′) and IN 2R (3′-CCTAGTGGGATGTGTACTTCTGAACTTA-3′) for *IN*, and IN 2F and F for *IN*–gp120. The PCR conditions used were as described above. The second-round PCR products were purified and cloned into a pGEM-T Easy Vector (Promega) or pCR-XL-TOPO Vector (Invitrogen), and the *env* and *IN* regions in both the passaged and selected viruses were sequenced using an Applied Biosystems 3500xL Genetic Analyzer and a BigDye Terminator v3.1 Cycle Sequencing kit (Applied Biosystems). Phylogenetic reconstructions were generated using the neighbour-joining method embedded in the MEGA software (http://www.megasoftware.net) (Tamura *et al.*, 2007). Overall, mean distances for viral diversity were also calculated using MEGA software. The number and location of putative PNGs were estimated using *N*-GlycoSite (http://www.hiv.lanl.gov/content/sequence/GLYCOSITE/glycosite.html) from the Los Alamos National Laboratory database.

Susceptibility assay. The sensitivity of the passaged viruses to various drugs was determined as described previously with minor modifications (Hatada *et al.*, 2010; Shibata *et al.*, 2007; Yoshimura *et al.*, 2006, 2010b). Briefly, PM1/CCR5 cells (2×10^3 cells per well) in 96-well round-bottomed plates were exposed to 100 $TCID_{50}$ of the viruses in the presence of various concentrations of drugs and incubated at 37 °C for 7 days. The IC_{50} values were then determined using a Cell Counting Kit-8 assay (Dojindo Laboratories). All assays were performed in duplicate or triplicate.

Predicting co-receptor usage by the V3 sequence. HIV-1 tropism was inferred using Geno2pheno [coreceptor] program, with a false rate positive (FPR) value of 5.0 %, which is freely available (http://coreceptor.bioinf.mpi-inf.mpg.de/index.php). This genotyping tool more accurately predicts virological responses to the CCR5 antagonist MVC in ARV-naïve patients than a reference phenotypic tropism test (Sing *et al.*, 2007).

Statistical analyses. Pairwise comparisons of the different parameters between variants in the two groups was calculated using the homoscedastic *t*-test. A P value of <0.05 was considered statistically significant.

ACKNOWLEDGEMENTS

We are grateful to Dr Yosuke Maeda for providing the PM1/CCR5 cells. We also thank Syoko Yamashita, Yoko Kawanami, Noriko Shirai and Akiko Shibata for technical assistance. This study was supported in part by the Ministry of Education, Culture, Sports, Science and Technology, Japan, by a Grant-in-Aid for Young Scientists (B-22790163); grants from the Ministry of Health, Labour and Welfare; the Program of Founding Research Centers for Emerging and Re-emerging Infectious Diseases; and the Global COE program Global Education and Research Center Aiming at the Control of AIDS.

REFERENCES

Anastassopoulou, C. G., Ketas, T. J., Klasse, P. J. & Moore, J. P. (2009). Resistance to CCR5 inhibitors caused by sequence changes in the fusion peptide of HIV-1 gp41. *Proc Natl Acad Sci U S A* **106**, 5318–5323.

Berro, R., Sanders, R. W., Lu, M., Klasse, P. J. & Moore, J. P. (2009). Two HIV-1 variants resistant to small molecule CCR5 inhibitors differ in how they use CCR5 for entry. *PLoS Pathog* **5**, e1000548.

Charpentier, C., Nora, T., Tenaillon, O., Clavel, F. & Hance, A. J. (2006). Extensive recombination among human immunodeficiency virus type 1 quasispecies makes an important contribution to viral diversity in individual patients. *J Virol* **80**, 2472–2482.

Delwart, E. L., Pan, H., Neumann, A. & Markowitz, M. (1998). Rapid, transient changes at the *env* locus of plasma human immunodeficiency virus type 1 populations during the emergence of protease inhibitor resistance. *J Virol* **72**, 2416–2421.

Eigen, M. (1993). The origin of genetic information: viruses as models. *Gene* **135**, 37–47.

Gulick, R. M., Lalezari, J., Goodrich, J., Clumeck, N., DeJesus, E., Horban, A., Nadler, J., Clotet, B., Karlsson, A. & other authors (2008). Maraviroc for previously treated patients with R5 HIV-1 infection. *N Engl J Med* **359**, 1429–1441.

Hatada, M., Yoshimura, K., Harada, S., Kawanami, Y., Shibata, J. & Matsushita, S. (2010). Human immunodeficiency virus type 1 evasion of a neutralizing anti-V3 antibody involves acquisition of a potential glycosylation site in V2. *J Gen Virol* **91**, 1335–1345.

Hombrouck, A., Voet, A., Van Remoortel, B., Desadeleer, C., De Maeyer, M., Debyser, Z. & Witvrouw, M. (2008). Mutations in human immunodeficiency virus type 1 integrase confer resistance to the naphthyridine L-870,810 and cross-resistance to the clinical trial drug GS-9137. *Antimicrob Agents Chemother* **52**, 2069–2078.

Ibáñez, A., Clotet, B. & Martínez, M. A. (2000). Human immunodeficiency virus type 1 population bottleneck during indinavir therapy causes a genetic drift in the env quasispecies. *J Gen Virol* **81**, 85–95.

Jacobson, J. M., Thompson, M. A., Lalezari, J. P., Saag, M. S., Zingman, B. S., D'Ambrosio, P., Stambler, N., Rotshteyn, Y., Marozsan, A. J. & other authors (2010). Anti-HIV-1 activity of weekly or biweekly treatment with subcutaneous PRO 140, a CCR5 monoclonal antibody. *J Infect Dis* **201**, 1481–1487.

Kitrinos, K. M., Nelson, J. A., Resch, W. & Swanstrom, R. (2005). Effect of a protease inhibitor-induced genetic bottleneck on human immunodeficiency virus type 1 *env* gene populations. *J Virol* **79**, 10627–10637.

Kobayashi, M., Nakahara, K., Seki, T., Miki, S., Kawauchi, S., Suyama, A., Wakasa-Morimoto, C., Kodama, M., Endoh, T. & Oosugi, E. (2008). Selection of diverse and clinically relevant integrase inhibitor-resistant human immunodeficiency virus type 1 mutants. *Antiviral Res* **80**, 213–222.

Maeda, Y., Yusa, K. & Harada, S. (2008). Altered sensitivity of an R5X4 HIV-1 strain 89.6 to coreceptor inhibitors by a single amino acid substitution in the V3 region of gp120. *Antiviral Res* **77**, 128–135.

McNicholas, P., Wei, Y., Whitcomb, J., Greaves, W., Black, T. A., Tremblay, C. L. & Strizki, J. M. (2010). Characterization of emergent HIV resistance in treatment-naive subjects enrolled in a vicriviroc phase 2 trial. *J Infect Dis* **201**, 1470–1480.

Nájera, R., Delgado, E., Pérez-Alvarez, L. & Thomson, M. M. (2002). Genetic recombination and its role in the development of the HIV-1 pandemic. *AIDS* **16** (Suppl. 4), S3–S16.

Nettles, R., Schurmann, D., Zhu, L., Stonier, M., Huang, S. P., Chien, C., Krystal, M., Wind-Rotolo, M., Bertz, R. & Grasela, D. (2011). Pharmacodynamics, safety, and pharmacokinetics of BMS-663068: a potentially first-in-class oral HIV attachment inhibitor. In *18th Conference on Retroviruses and Opportunistic Infections*, abstract 49. Boston, MA.

Nijhuis, M., Boucher, C. A., Schipper, P., Leitner, T., Schuurman, R. & Albert, J. (1998). Stochastic processes strongly influence HIV-1 evolution during suboptimal protease-inhibitor therapy. *Proc Natl Acad Sci U S A* **95**, 14441–14446.

Nora, T., Charpentier, C., Tenaillon, O., Hoede, C., Clavel, F. & Hance, A. J. (2007). Contribution of recombination to the evolution of human immunodeficiency viruses expressing resistance to antiretroviral treatment. *J Virol* **81**, 7620–7628.

Rhee, S.-Y., Liu, T. F., Kiuchi, M., Zioni, R., Gifford, R. J., Holmes, S. P. & Shafer, R. W. (2008). Natural variation of HIV-1 group M integrase: implications for a new class of antiretroviral inhibitors. *Retrovirology* **5**, 74.

Sheehy, N., Desselberger, U., Whitwell, H. & Ball, J. K. (1996). Concurrent evolution of regions of the envelope and polymerase genes of human immunodeficiency virus type 1 observed during zidovudine (AZT) therapy. *J Gen Virol* **77**, 1071–1081.

Shibata, J., Yoshimura, K., Honda, A., Koito, A., Murakami, T. & Matsushita, S. (2007). Impact of V2 mutations on escape from a potent neutralizing anti-V3 monoclonal antibody during in vitro selection of a primary human immunodeficiency virus type 1 isolate. *J Virol* **81**, 3757–3768.

Sing, T., Low, A. J., Beerenwinkel, N., Sander, O., Cheung, P. K., Domingues, F. S., Büch, J., Däumer, M., Kaiser, R. & other authors (2007). Predicting HIV coreceptor usage on the basis of genetic and clinical covariates. *Antivir Ther* **12**, 1097–1106.

Steigbigel, R. T., Cooper, D. A., Kumar, P. N., Eron, J. E., Schechter, M., Markowitz, M., Loutfy, M. R., Lennox, J. L., Gatell, J. M. & other authors (2008). Raltegravir with optimized background therapy for resistant HIV-1 infection. *N Engl J Med* **359**, 339–354.

Stupple, P. A., Batchelor, D. V., Corless, M., Dorr, P. K., Ellis, D., Fenwick, D. R., Galan, S. R., Jones, R. M., Mason, H. J. & other authors (2011). An imidazopiperidine series of CCR5 antagonists for the treatment of HIV: the discovery of N-(1S)-1-(3-fluorophenyl)-3-[(3-endo)-3-(5-isobutyryl-2-methyl-4,5,6,7-tetrahydro-1H-imidazo[4,5-c]pyridin-1-yl)-8-azabicyclo[3.2.1]oct-8-yl]propylacetamide (PF-232798). *J Med Chem* **54**, 67–77.

Tamura, K., Dudley, J., Nei, M. & Kumar, S. (2007). MEGA4: Molecular Evolutionary Genetics Analysis (MEGA) software version 4.0. *Mol Biol Evol* **24**, 1596–1599.

Tilton, J. C., Wilen, C. B., Didigu, C. A., Sinha, R., Harrison, J. E., Agrawal-Gamse, C., Henning, E. A., Bushman, F. D., Martin, J. N. & other authors (2010). A maraviroc-resistant HIV-1 with narrow cross-resistance to other CCR5 antagonists depends on both N-terminal and extracellular loop domains of drug-bound CCR5. *J Virol* **84**, 10863–10876.

Toma, J., Weinheimer, S. P., Stawiski, E., Whitcomb, J. M., Lewis, S. T., Petropoulos, C. J. & Huang, W. (2011). Loss of asparagine-linked glycosylation sites in variable region 5 of human immunodeficiency virus type 1 envelope is associated with resistance to CD4 antibody ibalizumab. *J Virol* **85**, 3872–3880.

Vignuzzi, M., Stone, J. K., Arnold, J. J., Cameron, C. E. & Andino, R. (2006). Quasispecies diversity determines pathogenesis through cooperative interactions in a viral population. *Nature* **439**, 344–348.

Yoshimura, K., Shibata, J., Kimura, T., Honda, A., Maeda, Y., Koito, A., Murakami, T., Mitsuya, H. & Matsushita, S. (2006). Resistance profile of a neutralizing anti-HIV monoclonal antibody, KD-247, that shows favourable synergism with anti-CCR5 inhibitors. *AIDS* **20**, 2065–2073.

Yoshimura, K., Harada, S., Hatada, M. & Matsushita, S. (2009). Mutations in V4 and C4 regions of the HIV-1 CRF08-BC envelope induced by the in vitro selection of Maraviroc Confer cross-resistance to other CCR5 inhibitors. In *16th Conference on Retroviruses and Opportunistic Infections*, p. 640. Montreal, Canada.

Yoshimura, K., Harada, S. & Matsushita, S. (2010a). Two step escape pathway of the HIV-1 subtype C primary isolate induced by the in vitro selection of Maraviroc. In *17th Conference on Retroviruses and Opportunistic Infections*, abstract 535. San Francisco, CA.

Yoshimura, K., Harada, S., Shibata, J., Hatada, M., Yamada, Y., Ochiai, C., Tamamura, H. & Matsushita, S. (2010b). Enhanced exposure of human immunodeficiency virus type 1 primary isolate neutralization epitopes through binding of CD4 mimetic compounds. *J Virol* **84**, 7558–7568.

Yusa, K., Maeda, Y., Fujioka, A., Monde, K. & Harada, S. (2005). Isolation of TAK-779-resistant HIV-1 from an R5 HIV-1 GP120 V3 loop library. *J Biol Chem* **280**, 30083–30090.

Zhang, Y. M., Dawson, S. C., Landsman, D., Lane, H. C. & Salzman, N. P. (1994). Persistence of four related human immunodeficiency virus subtypes during the course of zidovudine therapy: relationship between virion RNA and proviral DNA. *J Virol* **68**, 425–432.

frontiers in
MICROBIOLOGY

ORIGINAL RESEARCH ARTICLE
published: 14 May 2013
doi: 10.3389/fmicb.2013.00117

Increased infectivity in human cells and resistance to antibody-mediated neutralization by truncation of the SIV gp41 cytoplasmic tail

*Takeo Kuwata[1], Kaori Takaki[1], Ikumi Enomoto[1], Kazuhisa Yoshimura[2] and Shuzo Matsushita[1]**

[1] Center for AIDS Research, Kumamoto University, Kumamoto, Japan
[2] AIDS Research Center, National Institute of Infectious Diseases, Tokyo, Japan

Edited by:
Akio Adachi, The University of Tokushima Graduate School, Japan

Reviewed by:
Tetsuro Matano, University of Tokyo, Japan
Tsutomu Murakami, National Institute of Infectious Diseases, Japan
Hirofumi Akari, Kyoto University, Japan

***Correspondence:**
Shuzo Matsushita, Center for AIDS Research, Kumamoto University, 2-2-1 Honjo, Chuo-ku, Kumamoto 860-0811, Japan.
e-mail: shuzo@kumamoto-u.ac.jp

The role of antibodies in protecting the host from human immunodeficiency virus type 1 (HIV-1) infection is of considerable interest, particularly because the RV144 trial results suggest that antibodies contribute to protection. Although infection of non-human primates with simian immunodeficiency virus (SIV) is commonly used as an animal model of HIV-1 infection, the viral epitopes that elicit potent and broad neutralizing antibodies to SIV have not been identified. We isolated a monoclonal antibody (MAb) B404 that potently and broadly neutralizes various SIV strains. B404 targets a conformational epitope comprising the V3 and V4 loops of Env that intensely exposed when Env binds CD4. B404-resistant variants were obtained by passaging viruses in the presence of increasing concentration of B404 in PM1/CCR5 cells. Genetic analysis revealed that the Q733stop mutation, which truncates the cytoplasmic tail of gp41, was the first major substitution in Env during passage. The maximal inhibition by B404 and other MAbs were significantly decreased against a recombinant virus with a gp41 truncation compared with the parental SIVmac316. This indicates that the gp41 truncation was associated with resistance to antibody-mediated neutralization. The infectivities of the recombinant virus with the gp41 truncation were 7,900-, 1,000-, and 140-fold higher than those of SIVmac316 in PM1, PM1/CCR5, and TZM-bl cells, respectively. Immunoblotting analysis revealed that the gp41 truncation enhanced the incorporation of Env into virions. The effect of the gp41 truncation on infectivity was not obvious in the HSC-F macaque cell line, although the resistance of viruses harboring the gp41 truncation to neutralization was maintained. These results suggest that viruses with a truncated gp41 cytoplasmic tail were selected by increased infectivity in human cells and by acquiring resistance to neutralizing antibody.

Keywords: SIV, gp41, truncation, infectivity, resistance, neutralization, antibody

INTRODUCTION

The RV144 trial demonstrated 31% vaccine efficacy for preventing human immunodeficiency virus type 1 (HIV-1) infection (Rerks-Ngarm et al., 2009). Antibodies against the HIV-1, particularly against the V1/V2 loops, correlate inversely with infection risk (Haynes et al., 2012). Further recent isolation of monoclonal antibodies (MAbs) that neutralize a broad range of HIV-1 strains suggest the possibility for developing a vaccine that can induce cross-neutralizing antibodies effective for various HIV-1 strains (Kwong and Mascola, 2012). Although non-human primate models of simian immunodeficiency virus (SIV) infection can facilitate the evaluation of immunogens, epitopes and immune correlates, no potent and broad neutralizing MAb against SIV had been available.

To understand the mechanisms involved in neutralization of infectivity by antibodies in an SIV model, we recently isolated MAb B404 from a SIVsmH635FC-infected rhesus macaque, which potently and broadly neutralizes various SIV strains, such as SIVsmE543-3, SIVsmE660 and the neutralization-resistant variants, genetically diverse SIVmac316, and highly neutralization-resistant SIVmac239 (Kuwata et al., 2011). The B404 epitope, which comprises the V3 and V4 loops of Env and is intensely exposed by ligation of Env to CD4, is the target for potent and broad neutralization of SIV (Kuwata et al., 2013). Vigorous induction of B404-like neutralizing antibodies using the specific VH3 gene with a long complementarity-determining region 3 loop and λ light chain was observed in four SIVsmH635FC-infected macaques. The B404-resistant variants were induced by passaging viruses in the presence of increasing concentrations of B404. Genetical analysis of the gp120 region of B404-resistant variants revealed that the mutations in the C2 region of Env were important for the resistance to antibody-mediated neutralization (Kuwata et al., 2013).

In the present study, we further analyzed B404-resistant variants and determined the precise region responsible for the resistance to antibody-mediated neutralization. Genetic analysis of viruses during passage in the presence of B404 as well as phenotypic analysis using recombinant viruses revealed that a truncation of the gp41 cytoplasmic tail was the primary step leading to escape from neutralization.

MATERIALS AND METHODS

CELLS

PM1 (Lusso et al., 1995), PM1/CCR5 (Yusa et al., 2005), and HSC-F (Akari et al., 1999) cells were maintained in Roswell Park Memorial Institute (RPMI) 1640 medium containing 10% fetal bovine serum (FBS). TZM-bl (Platt et al., 1998; Derdeyn et al., 2000; Wei et al., 2002; Takeuchi et al., 2008) and 293T (DuBridge et al., 1987) cells were maintained in Dulbecco's modified Eagle's medium containing 10% FBS.

GENETIC ANALYSIS OF B404-RESISTANT VARIANTS

The induction of variants resistant to Fab-B404 (Kuwata et al., 2011) from SIVmac316 (Mori et al., 1992) harboring full-length gp41 was performed as described previously (Yoshimura et al., 2006; Hatada et al., 2010; Kuwata et al., 2013). Briefly, 5,000 $TCID_{50}$ (50% tissue culture infectious dose) SIVmac316 was incubated with 5 ng/ml Fab-B404 for 30 min at 37°C. Then, 5×10^4 PM1/CCR5 cells were added to the virus–Fab mixture. After incubation for 5 h, cells were washed with phosphate-buffered saline (PBS) and resuspended in RPMI 1640 supplemented with 10% FBS without Fab-B404. The culture supernatant was harvested 7 days later and used to infect fresh PM1/CCR5 cells for the next round of culture in the presence of increasing concentrations of Fab-B404. Proviral DNA samples were extracted from cells using a QIAamp DNA Blood Mini Kit (QIAGEN, Hilden, Germany) after 8, 17, 20, 23, and 26 passages as well as from P26C cells obtained after 26 passages in the absence of Fab-B404. The gp120 region was amplified using Platinum Taq DNA Polymerase High Fidelity (Invitrogen, Carlsbad, CA, USA) with primers SEnv-F (5′-ATG GGA TGT CTT GGG AAT CAG C-3′) and SER1 (5′-CCA AGA ACC CTA GCA CAA AGA CCC-3′). The whole *env* gene was amplified with primers SRev-F (5′-GGT TTG GGA ATA TGC TAT GAG-3′) and SEnv-R (5′-CCT ACT AAG TCA TCA TCT T-3′). The polymerase chain reaction (PCR) products were cloned using a TA cloning kit (Invitrogen), and subjected to sequencing. Nucleotide sequences were aligned and analyzed phylogenetically using Molecular Evolutionary Genetics Analysis version 5 (MEGA5) (Tamura et al., 2011).

CONSTRUCTION OF INFECTIOUS MOLECULAR CLONES WITH THE Env REGION FROM B404-RESISTANT VARIANTS

One of the clones from passage 26, P26B404 clone 26, was selected for construction of recombinant viruses, because this clone had mutations typical of the major population of P26B404 variants. Infectious molecular clones SS, SN, and NS were generated by replacing fragments *Sph*I–*Sac*I [nucleotides (nt) 6,446–9,226], *Sph*I–*Nhe*I (nt 6,446–8,742), and *Nhe*I–*Sac*I (nt 8,742–9,226) with the corresponding regions of SIVmac316, respectively. Mutants F277V and N295S, which have point mutations at amino acid residues 277 and 295 of Env, respectively, were constructed by PCR mutagenesis using the SIVmac316 plasmid as template. The changes from phenylalanine (TTC) to valine (GTC) in F277V and asparagine (AAT) to serine (AGT) in N295S were introduced using primers F277VFw (5′-TTG GTT TGG CGT CAA TGG TAC TAG GGC-3′), F277VRv (5′-GTA CCA TTG ACG CCA AAC CAA G-3′), N295SFw (5′-GGC AAT AGT AGT AGA ACC ATA ATT AG-3′), and N295SRv (5′-AAT TAT GGT TCT ACT ACT ATT GCC-3′). Mutant and parental SIVmac316 plasmids were transfected into 293T cells using X-tremeGENE 9 DNA Transfection Reagent (Roche Molecular Biochemicals, Mannheim, Germany). After 2 days, the supernatants containing viruses were filtered (0.45 μm) and stored at −80°C.

ANALYSIS OF VIRAL INFECTIVITY

For determination of $TCID_{50}$ in PM1 and PM1/CCR5 cells, 5×10^4 cells in 50 μl were inoculated with 50 μl serially diluted virus stocks in a 96-well plate and cultured for 2 weeks. Virus replication was judged by observation of cytopathic effects (CPE) by light microscopy. The $TCID_{50}$ in TZM-bl cells was determined by measuring luciferase activities. Briefly, 100 μl medium, 50 μl serially diluted virus stock, and 50 μl 1×10^4 cells containing 37.5 μg/ml diethylaminoethyl (DEAE) dextran were added to the wells of a 96-well plate. The plate was then incubated at 37°C for 2 days. After washing with PBS, cells were lysed with 30 μl cell lysing buffer (Promega, Madison, WI, USA) for 15 min at room temperature (RT) and then 10 μl of cell lysate was transferred to a 96-well white solid plate (Coster, Cambridge, MA, USA). Luciferase activity was measured using a Centro XS3 LB960 microplate luminometer (Berthold Technologies, Bad Wildbad, Germany) and a luciferase assay system (Promega). The $TCID_{50}$ was calculated according to the formula of Reed and Muench (1938).

Infectivity of viruses in PM1, PM1/CCR5, and HSC-F cells was evaluated by detecting infected cells using flow cytometry as described previously (Kuwata et al., 2011). Briefly, PM1 and PM1/CCR5 cells were adjusted to 1×10^6 cells/ml and HSC-F cells were adjusted to 5×10^6 cells/ml. Aliquots of 100 μl cells per well in a 24-well plate were inoculated with 100 μl of diluted virus stocks. After incubation for 6 h, 800 μl fresh medium was added to wells. One-half of the cells in each well were collected at 4, 7, and 10 days post-inoculation. Cells were washed with PBS and fixed with IC Fixation Buffer (eBioscience, San Diego, CA, USA). After washing with Permeabilization Buffer (eBioscience) twice, the cells were intracellularly stained with 4 μg/ml (50 μl) anti-p27 Fab, B450 (Kuwata et al., 2011) by incubation for 20 min at RT. The cells were then incubated with 50 μl anti-HA antibody (1:200; 3F10, Roche Molecular Biochemicals) for 20 min at RT followed by incubation with 50 μl of anti-rat-FITC (1:500; Santa Cruz Biotechnology, Santa Cruz, CA, USA) for 20 min at RT. The stained cells were analyzed using a FACSCalibur (BD Biosciences, Franklin Lakes, NJ, USA). Frequencies of infected cells were determined by comparison with an uninfected control. Data analysis was performed using FlowJo (TreeStar, San Carlos, CA, USA).

All infectivity experiments were performed at least twice and the representative results are shown.

ANALYSIS OF NEUTRALIZING ACTIVITIES

The Fab clones B404 and K8, isolated from an SIV-infected macaque (Kuwata et al., 2011), and murine MAb M318T (Matsumi et al., 1995) were used to examine the sensitivity of viruses to antibody-mediated neutralization in TZM-bl cells as described previously (Kuwata et al., 2011). Briefly, 100 μl serially diluted antibodies in duplicate were incubated with 200 $TCID_{50}$ (50 μl) of virus in a 96-well plate. After incubation for 1 h at 37°C, 100 μl

of 1×10^5 TZM-bl cells/ml containing 37.5 μg/ml DEAE dextran were added. After incubation for 2 days, luciferase activities were measured as described above for the analysis of viral infectivity. The 50% inhibitory concentrations (IC_{50}) and maximal percent of inhibition (MPI) were calculated from the average values by non-linear regression using Prism5 (GraphPad Software, San Diego, CA, USA).

Sensitivity to neutralization by B404 in macaque cells was analyzed using HSC-F cells, a cynomolgus macaque cell line immortalized by infection with *Herpesvirus saimiri* (Akari et al., 1999). Fab-B404 was serially diluted and 50 μl aliquots were mixed with 50 μl undiluted or 10-fold diluted virus in a 96-well plate. After 1 h incubation at 37°C, 2×10^5 cells in 100 μl were added to each well and cultured for 1 day. The infected cells were washed twice with PBS, resuspended in 200 μl fresh medium, and cultured in a new 96-well plate. Viral infection was examined 4 days post-inoculation by intracellular staining of p27, as described above for the analysis of viral infectivity. Infectivity was determined in duplicate and the average value was used for the analysis of neutralization.

All neutralizing assays were performed at least twice and the representative results are shown.

WESTERN BLOTTING ANALYSIS OF VIRAL PROTEINS

Cells and supernatants were collected from six-well plate 2 days after transfection of 293T cells with infectious molecular clones, as previously described (Yuste et al., 2005). Supernatants were filtered (0.45 μm) and clarified by centrifugation for 10 min at 3,000 rpm. The clarified supernatants were centrifuged at 13,200 rpm for 90 min at 4°C, and the viral pellets were resuspended in 1 ml PBS and centrifuged again. Pellets were then dissolved in 80 μl sample buffer [62.5 mM Tris–HCl, pH 6.8, 2% sodium dodecyl sulfate (SDS), 25% glycerol, 5% 2-mercaptoethanol, 0.01% bromophenol blue]. Cells were washed with PBS and lysed in 300 μl sample buffer. Samples of virions and cell lysates were boiled for 5 min, and the proteins were separated by SDS-polyacrylamide gel electrophoresis using SuperSep Ace 5–20% (Wako Pure Chemical Industries, Osaka, Japan). Proteins were transferred to an Immun-Blot PVDF Membrane (Bio-Rad Laboratories, Hercules, CA, USA). The membrane was blocked with 5% skim milk TBS-T (Tris-buffered saline containing 0.1% Tween 20) for 1 h at RT, and then washed three times with TBS-T. For the detection of gp120, the membrane was incubated overnight at 4°C with 1 μg/ml M318T (Matsumi et al., 1995) in 5% skim milk TBS-T. After washing three times with TBS-T, the membrane was incubated with anti-mouse immunoglobulin G (IgG) peroxidase (1:4,000, Santa Cruz Biotechnology) for 1 h at RT. The membrane was washed three times with TBS-T and once with TBS, and then TMB solution (KPL, Gaithersburg, MD, USA) was added to develop color. Viral proteins gp41 and p26 were similarly examined using crude supernatants from bacterial culture producing B408 and B450 (Kuwata et al., 2011), which were mixed with the same amount of 5% skim milk TBS-T. The membrane was incubated with anti-HA-HRP antibody (1:1,000; Roche Molecular Biochemicals) and Chemi-Lumi One L (Nacalai Tesque, Kyoto, Japan), and viral proteins were visualized using ImageQuant LAS 4000 (GE Healthcare, Piscataway, NJ, USA)

RESULTS

EVOLUTION OF VIRUSES DURING PASSAGE UNDER THE PRESSURE OF Fab-B404

To select for variants resistant to MAb B404, an antibody that targets a conformational epitope comprising the gp120 V3 and V4 loops, we passaged SIVmac316 that possesses a full-length gp41 in PM1/CCR5 cells in the presence of increasing concentrations of Fab-B404. The virus recovered at passage 26 (P26B404) was resistant to neutralization by B404 (V3/V4) and other antibodies, MAbs K8 (CD4i) and M318T (V2), that target epitopes other than that recognized by B404 (Kuwata et al., 2013). The region covering the whole *env* gene were amplified by PCR and cloned from viruses at passage 8, 17, 20, 23, and 26. The nucleotide sequences were phylogenetically analyzed to show the evolution of B404-resistant variants (**Figure 1**). The first major mutation was a change from glutamine (CAG) to a stop codon (TAG) at 733rd amino acid residue of Env. The Q733stop substitution in the gp41 cytoplasmic domain was observed in 12 of 14 clones at passage 8 and in all clones thereafter. Another stop codon (W782stop) was the second

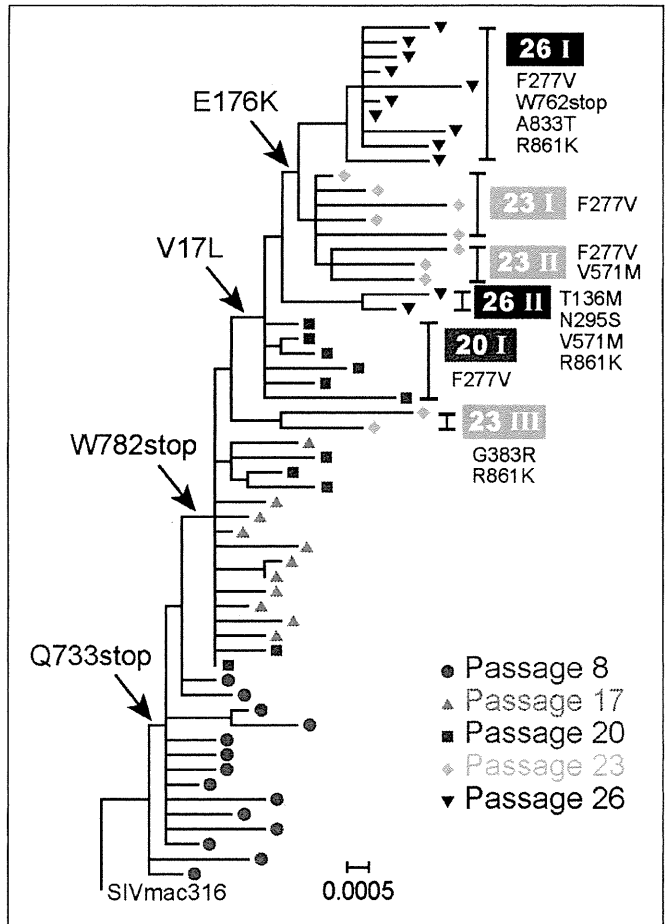

FIGURE 1 | Evolution of B404-resistant variants. Nucleotide sequences of the *env* gene, which were derived from proviruses at passages 8, 17, 20, 23, and 26, were phylogenetically analyzed using MEGA5. Arrows indicate major substitutions as follows: Q733stop, W782stop, V17L, and E176K. Clones with representative amino acid substitutions were separated into groups, which are shown on the right side along with the corresponding substitutions.

major mutation, which was detected after 17 passages. Substitutions V17L in the signal peptide and E176K in the V2 loop emerged after 20 and 23 passages, respectively, although the E176K substitution was also observed in P26C, control viruses after 26 passages in the absence of B404 (**Table 1**). In addition to these substitutions, most of clones acquired the F277V substitution in the late stage of evolution, except for one group at passage 26 which has the N295S substitution (see **Figure 1**, group 26II). Group 26II was clearly distinguished from group 26I by amino acid substitutions, such as T136M, N295S, and D571M/E (**Table 1**), suggesting two lineages of variants in P26B404.

These results demonstrated that the first step in acquiring resistance to B404 was the truncation of gp41. Although substitutions in gp120, represented by F277V, might contribute to the resistance to a high concentration of B404, 20 passages were required for the emergence of these substitutions.

Table 1 | Frequency* of amino acid substitutions in Env clones from B404-resistant variants after 26 passages.

Substitution	Region	P26B404		P26C
		I	II	
	gp120	**(*n* = 22)**	**(*n* = 8)**	**(*n* = 14)**
V17L	Signal peptide	**100%**	**100%**	0.0%
G62S	C1	0.0%	0.0%	21.4%
M67V/L/T	C1	4.5%	0.0%	21.4%
A68T	C1	0.0%	0.0%	**92.9%**
T136M	V1	4.5%	**87.5%**	0.0%
T137I	V1	0.0%	0.0%	14.3%
K141E/R	V1	0.0%	12.5%	7.1%
E176K	V2	**90.9%**	12.5%	35.7%
F277V	C2	**100%**	0.0%	0.0%
N295S	C2	0.0%	**100%**	0.0%
Q341H	V3	13.6%	12.5%	14.3%
D374N	C3	0.0%	0.0%	28.6%
K403R	V4	0.0%	12.5%	7.1%
W441R	C4	4.5%	0.0%	7.1%
	gp41	**(*n* = 10)**	**(*n* = 2)**	**(*n* = 7)**
F528S/L	Extracellular	20.0%	0.0%	0.0%
D571M/E	Extracellular	10.0%	**100%**	0.0%
Q733stop	Cytoplasmic	**100%**	**100%**	0.0%
W762stop	Cytoplasmic	**100%**	0.0%	0.0%
W782stop	Cytoplasmic	**100%**	0.0%	0.0%
A833T	Cytoplasmic	**90.0%**	0.0%	0.0%
R839K	Cytoplasmic	0.0%	0.0%	**57.1%**
R861K	Cytoplasmic	**100%**	**100%**	0.0%

Percentages of substitutions in populations P26B404 and P26C, which were obtained after 26 passages in the presence and absence of B404, respectively, are shown. The P26B404 population is separated into two subpopulations according to the phylogenetic analysis in **Figure 1. All the substitutions that are observed in more than one clone are shown here. Boldface indicates substitutions dominant (>50%) in each population. The numbers of clones analyzed for the gp120 and gp41 regions are shown in parentheses.*

TRUNCATION OF gp41 CONFERRED RESISTANCE TO ANTIBODY-MEDIATED NEUTRALIZATION

To analyze effect of substitutions in B404-resistant variants on resistance to neutralization, recombinant viruses were constructed (**Figure 2**). The *env* region of SIVmac316 was replaced by that of P26B404 clone 26, which had substitutions typical to the P26I group. The resultant molecular clones SS, SN, and NS had substitutions in the entire *env* region, gp120 and gp41 from P26B404I, respectively. SS and NS were predicted to have a truncated gp41 with no other mutation in gp41, because the Q733stop substitution was the first substitution in gp41. Point mutants with substitutions F277V and N295S, which were representative mutations at late passages, were also constructed by PCR mutagenesis.

These mutant viruses were examined for their sensitivity to neutralization by three MAbs B404 (V3/V4 conformational), K8 (CD4i), and M318T (V2). The neutralization of SS that contain the entire *env* region from P26B404I was similar to those of P26B404, indicating that the *env* region is responsible for the

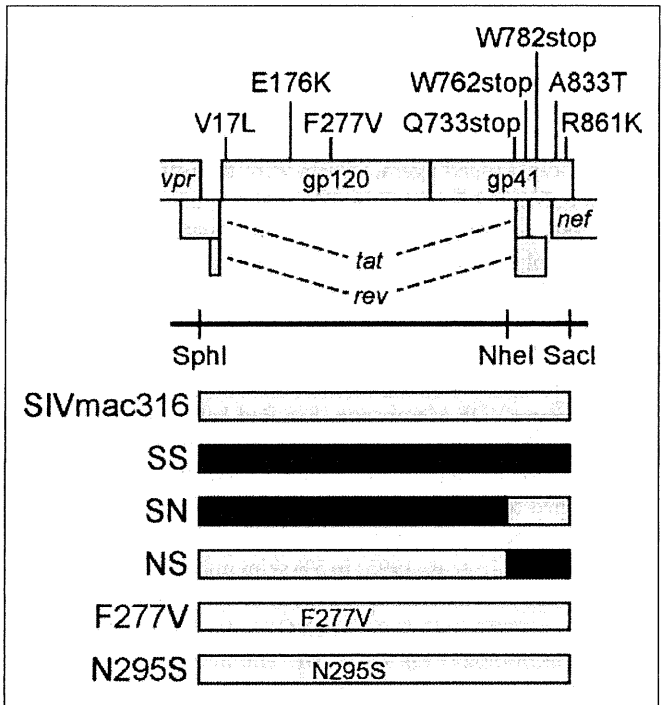

FIGURE 2 | Construction of infectious SIV clones with B404-resistant mutations. The open reading frames of the SIV genome are shown along with the Env substitutions in the B404-resistant variant typical to P26B404I. Full-length SIV clones were constructed from parental SIVmac316 by replacing the *env* region with that of the B404-resistant variant (blue) using *SphI*, *NheI*, and *SacI* sites. The resultant virus SS contains all of the Env substitutions present in P26B404I. Viruses SN and NS contain substitutions in gp120 and gp41, respectively. Point mutants F277V and N295S were constructed by inserting the substitutions F277V and N295S into SIVmac316, respectively.

resistance to neutralization (**Figure 3A**). Recombinants SN and NS, which have substitutions in gp120 and gp41 from P26B404I, respectively, showed varying degrees of resistance. The IC_{50} values of SN and NS against B404 were intermediates between the parental SIVmac316 and the neutralization-resistant P26B404. Maximal inhibition reached a plateau at 73.8, 82.3, and 81.9% in SS, NS, and P26B404, respectively, but the MPI value of SN (94.9%) was close to that of SIVmac316 (100%; **Figure 3B**). Neutralization resistance to anti-CD4i MAb K8 was characterized by decreases in the IC_{50} value of SN and the MPI of NS. Neutralization by anti-V2 MAb M318T was even enhanced in SN, although NS showed the resistance comparable to those of SS and P26B404. The decreases in MPI values were commonly observed for the neutralization of NS by the three MAbs (**Figure 3B**). Resistance to neutralization was not significantly detected by the point mutants F277V and N295S, except for the neutralization of F277V by K8 (4.3-fold decrease of IC_{50} value). These results indicated that the entire *env* region, including substitutions in both gp120 and gp41, was responsible for the full-resistance of P26B404 to neutralization. The decrease of MPI values for NS suggested that truncation of gp41 by the Q733stop substitution, the first major substitution in viral evolution, was important to escape from the neutralizing antibodies.

INCREASED INFECTIVITY FOR HUMAN CELLS BY SIV WITH A TRUNCATED gp41

Truncation of gp41 in SIV is associated with the adaptation to human cells (Hirsch et al., 1989; Kodama et al., 1989), which may partially contribute to neutralization resistance (Yuste et al., 2005). To explore the mechanism of neutralization resistance of P26B404, the infectivity of recombinant viruses was analyzed by determining the $TCID_{50}$ values of virus stocks prepared by transfection of 293T cells (**Table 2**). The $TCID_{50}$ values in all the human cells tested were significantly higher for SS and NS viruses with truncated gp41 than

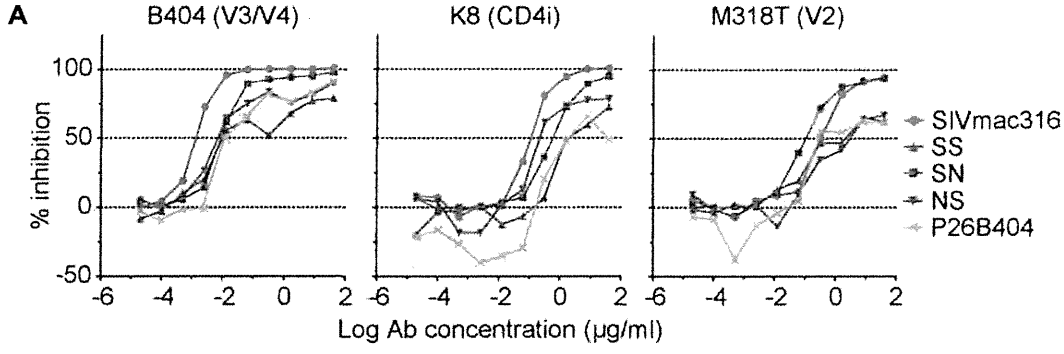

B

Neutralization profile of mutant viruses

Virus	B404 (V3/V4)		K8 (CD4i)		M318T (V2)	
	IC_{50}	MPI	IC_{50}	MPI	IC_{50}	MPI
SIVmac316	1.3E-03 (1.0)	100 (0.0)	1.1E-01 (1.0)	99.0 (0.0)	3.3E-01 (1.0)	94.3 (0.0)
SS	1.9E-02 (14.5)	73.8 (-26.2)	1.8E+00 (16.3)	67.9 (-31.1)	9.4E-01 (2.8)	65.5 (-28.8)
SN	9.1E-03 (6.8)	94.9 (-5.1)	5.9E-01 (5.3)	94.7 (-4.4)	1.0E-01 (0.3)	92.5 (-1.8)
NS	6.8E-03 (5.1)	82.3 (-17.7)	2.1E-01 (1.9)	77.0 (-22.0)	1.7E+00 (5.2)	67.6 (-26.7)
F277V	3.8E-03 (2.8)	100 (0.0)	4.8E-01 (4.3)	99.6 (0.5)	3.0E-01 (0.9)	94.8 (0.5)
N295S	2.3E-03 (1.7)	99.6 (-0.4)	1.4E-01 (1.2)	99.9 (0.8)	3.1E-01 (0.9)	97.0 (2.7)
P26B404	1.7E-02 (12.5)	81.9 (-18.1)	8.2E-01 (7.3)	54.6 (-44.5)	2.5E-01 (0.8)	60.0 (-34.3)

Fold change of IC_{50}
> 10
3-10
< 3

% change of MPI
< -20
-10 to -20
> -10

FIGURE 3 | Sensitivities of viruses with B404-resistant mutations to neutralization by MAbs. (A) Sensitivities of mutant viruses SS, SN, and NS to neutralization by MAbs Fab-B404 (anti-V3/V4), Fab-K8 (anti-CD4i), and M318T (anti-V2) are shown. Neutralization of parental SIVmac316 and B404-resistant P26B404 is also shown as controls sensitive and resistant to neutralization, respectively. **(B)** The sensitivities to neutralization are represented by values for IC_{50} (μg/ml) and MPI (%). Viruses were examined for their sensitivities to neutralization by MAbs Fab-B404, Fab-K8, and M318T in TZM-bl cells. The IC_{50} and MPI values were determined using Prism 5. The fold-change of IC_{50} was calculated by dividing the IC_{50} value by that of the parental SIVmac316. Percent change of MPI was calculated by subtracting the MPI value from that of SIVmac316. These changes are shown in parentheses and significant changes are indicated by magenta (IC_{50}: >10; MPI: < −20) and orange (IC_{50}: 3–10; MPI: −20 to −10) highlighting.

parental SIVmac316 and SN, in which gp41 is intact. In particular, NS showed a striking increase in $TCID_{50}$ values, which were 7,100-, 1,000-, and 140-fold higher than those of parental SIVmac316 in PM1, PM1/CCR5, and TZM-bl cells, respectively. These results indicate that truncation of gp41 caused by the Q733stop substitution increases viral infectivity for human cells.

To compare viral infectivity in human and macaque cells, viral infection was monitored after inoculation of PM1 and PM1/CCR5 human cells and the HSC-F cynomolgus macaque cell line with varying dilutions of virus stocks (**Figure 4**). Consistent with the $TCID_{50}$ analysis, a higher frequency of infected cells was detected earlier in PM1 and PM1/CCR5 cells inoculated with NS than the parental SIVmac316. In contrast, SN showed decreased infectivity in PM1 and PM1/CCR5 cells, apparently because PM1 cells were not infected by a 1,000-fold diluted SN stock. Although the $TCID_{50}$ values of SS were much higher than those of SIVmac316, the replication kinetics of SS were similar to those of SIVmac316 in PM1 and PM1/CCR5 cells. These results suggest that gp41 truncation increases infectivity for human cells and that the substitutions in gp120 of P26B404I are associated with slow and poor replication compared with that of SIVmac316.

Infectivity for macaque cells was more significantly affected than that for human cells by the substitutions in gp120 of P26B404I (**Figure 4**, lower panels). Infected cells were detected in HSC-F cells inoculated with 1,000-fold diluted virus stocks of SIVmac316 and NS, but viral infection in HSC-F cells was limited to a low frequency even by inoculation with 10-fold diluted virus stocks of SS and SN. Truncation of gp41 did not significantly affect replication in HSC-F macaque cells, although truncation of gp41 was disadvantageous for replication in primary T cell cultures from macaques (Hirsch et al., 1989; Kodama et al., 1989).

These results demonstrate that gp41 truncation strikingly increases infectivity for human cells, but not for macaque cells, and that the substitutions in gp120 decrease infectivity in human and macaque cells. Truncation of gp41, which conferred extremely high infectivity for PM1/CCR5 cells, may be the first step to escape from neutralization and the substitutions in gp120 may be the second step to replicate in the presence of high concentration of B404.

Table 2 | Infectivity* of viruses with substitutions from P26B404.

Viruses	PM1	PM1/CCR5	TZM-bl
SIVmac316	4.2E+02 (1.0)	1.4E+03 (1.0)	9.6E+04 (1.0)
SS	2.9E+05 (710)	4.7E+05 (350)	6.3E+06 (66)
SN	2.0E+03 (4.8)	8.4E+03 (6.2)	2.9E+05 (3.1)
NS	2.9E+06 (7,100)	1.4E+06 (1,000)	1.4E+07 (140)

**Infectivity is shown by the $TCID_{50}$/ml values of the viruses, which were prepared by transfection of 293T cells, in PM1, PM1/CCR5, and TZM-bl cells. The fold-change, which was calculated by dividing the mutant $TCID_{50}$/ml value by that of the parental SIVmac316, is shown in the parentheses.*

INCREASED INCORPORATION OF Env INTO VIRIONS IN SIV WITH TRUNCATED gp41

Incorporation of Env into virions was examined using these recombinant viruses, because increased infectivity by gp41 truncation was suggested to be associated with the Env content of virions (Manrique et al., 2001; Zhu et al., 2003, 2006; Yuste et al., 2004, 2005). Analysis of viral proteins in cells and supernatants from transfected 293T cells revealed that incorporation of Env into virions was significantly high in SS and NS viruses with the Q733stop substitution (**Figure 5**). MAb to gp120 showed a higher amount

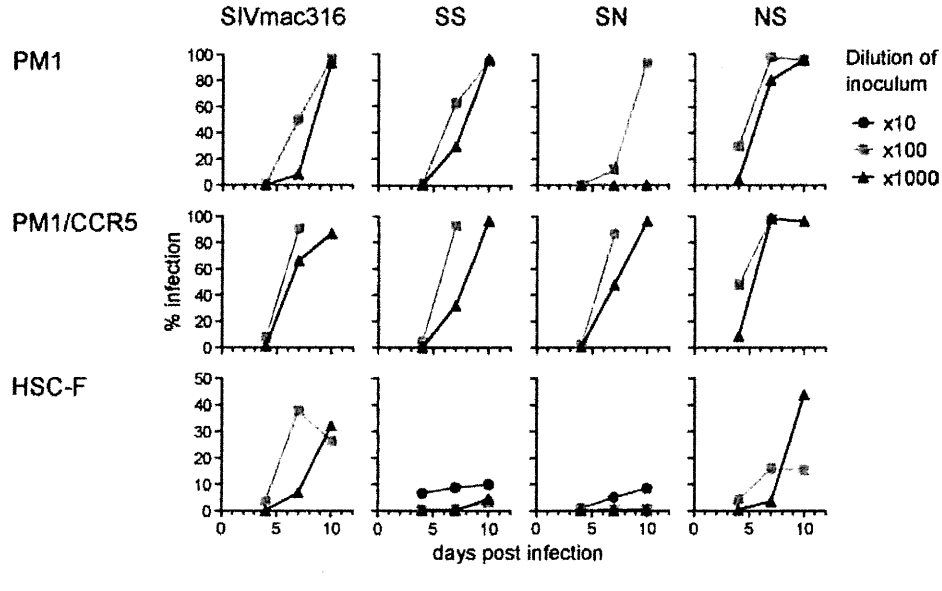

FIGURE 4 | Replication of B404-resistant viruses in human and macaque cells. Frequencies of infected cells at 4, 7, and 10 days post-infection are shown. PM1 and PM1/CCR5 human T cells and HSC-F cynomolgus macaque T cells were infected with the various dilutions of SIVmac316, SS, SN, and NS. Infected cells were detected using flow cytometry after intracellular staining by B450 (anti-p27 Fab).

of gp120 and gp160 in virions from SS and NS than those from SN and the parental SIVmac316, although the production of Env proteins in the transfected cells was at the same level among all the viruses (**Figure 5A**). MAb to gp41 also demonstrated that truncated gp41 was more abundant in virions compared with full-length gp41 (**Figure 5B**). Semi-quantification by densitometric scanning of gp41 and p26 images suggested that the levels of gp41 amount per virion in SS and NS were 12- and 44-fold higher than that of SIVmac316, respectively, after adjusting virion numbers using the p26 amounts. In contrast to the increased amount of Env proteins in virions from viruses with truncated gp41, the level of Gag p27 in virions was low in SS and NS compared with those in SN and SIVmac316 (**Figure 5C**). This indicates that the Env content per virion, which was normalized by the amount of p27, was significantly high in viruses with truncated gp41. These results suggest that truncation of gp41 by the Q733stop substitution enhances incorporation of Env into virions.

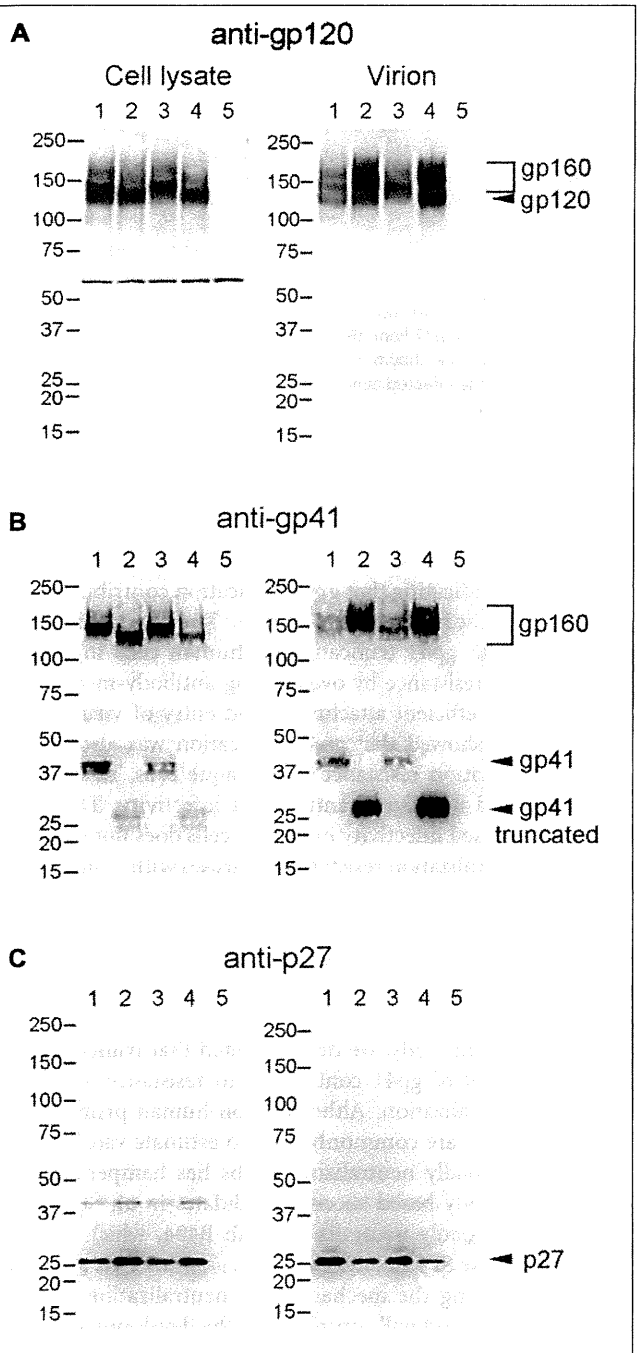

FIGURE 5 | Effect of B404-resistant mutations on the incorporation of Env into virions. Cell lysates (left panels) and virions (right panels) of SIVmac316 (lane 1), SS (lane 2), SN (lane 3), NS (lane 4), and mock-infected control (lane 5), which were prepared from transfected 293T cells, were analyzed by Western blotting. Viral proteins gp120 **(A)**, gp41 **(B)**, and p27 **(C)** were detected using MAbs M318T (anti-gp120 V2), B408 (anti-gp41 cluster I), and B450 (anti-p27), respectively.

NEUTRALIZATION RESISTANCE OF SIV WITH TRUNCATED gp41 IN MACAQUE CELLS

The analysis of infectivity of recombinant viruses suggested that the resistance to neutralization by truncation of gp41 might be due to adaptation to human cells. To examine this hypothesis, sensitivity to neutralization by B404 was determined in HSC-F macaque cells using SIVmac316 and NS, which showed similar infectivity for HSC-F cells (**Figure 4**). In flow cytometric analysis, infection in the presence or absence of B404 demonstrated that the high sensitivity of SIVmac316 and resistance of NS to neutralization were maintained in HSC-F cells (**Figure 6**). The frequency of infected cells decreased from 41.5% to the background level (2.03%) in inoculation with the undiluted stock of SIVmac316. In contrast, infection with NS, even with a 10-fold diluted virus stock, was significant in HSC-F cells in the presence of B404 (**Figure 6A**). Neutralization of NS in HSC-F cells was characterized by a decrease in maximal inhibition (**Figure 6B**), which was also observed in TZM-bl cells (**Figure 3A**). The magnitude of resistance of NS to B404 was greater when infection was performed using the undiluted stock compared with the 10-fold diluted stock, raising the possibility that B404 did not inhibit infection with a high titer of viruses. However, the resistance of NS was shown by infection with a low titer of NS, in which the frequency of infected cells in the absence of B404 (23.8%) was lower than infection with undiluted SIVmac316 (41.5%). Further, immunoblotting analysis revealed that the amount of virions was higher in the virus stock of SIVmac316 than that of NS (**Figure 5**).

These results indicate that gp41 truncation by the Q733stop substitution contributes to neutralization resistance of viruses in macaque cells. This suggests that the resistance to neutralization by truncation of gp41 is not due to the adaptation to human cells. The Q733stop substitution, the first major mutation during passages in the presence of B404, might be selected because it facilitates adaptation of virus to human cells and imparts resistance to antibody.

DISCUSSION

In the present study, truncation of the cytoplasmic tail of gp41, which was caused by the Q733stop substitution in Env, was the first major mutation detected during passage of SIV in the presence of the neutralizing antibody B404. Analysis of recombinant viruses suggested that the gp41 truncation was selected by their resistance to neutralizing antibody, which was characterized by the decrease of maximal inhibition compared with viruses with intact gp41, and

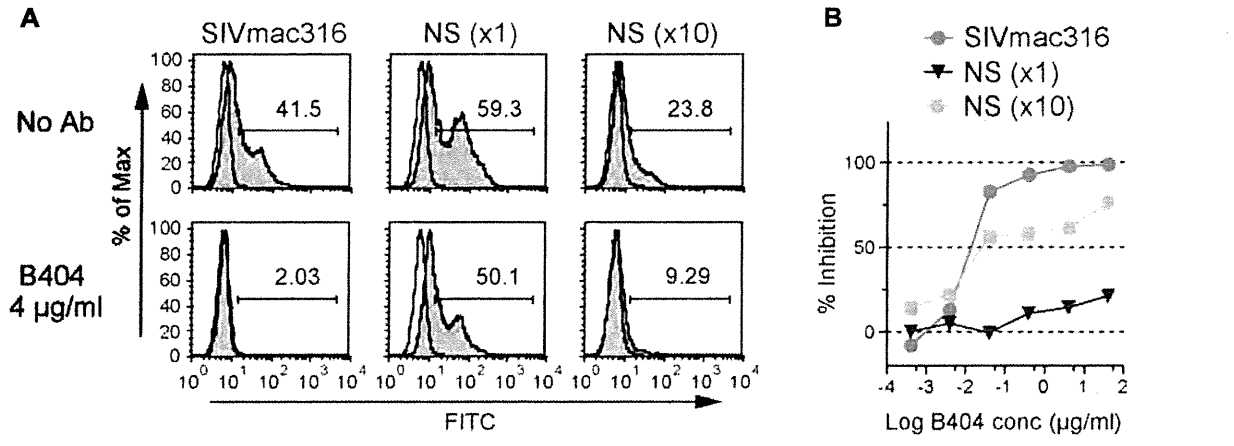

FIGURE 6 | Contribution of gp41 truncation to neutralization resistance in infection of macaque cells. (A) Infection of HSC-F cells in the presence (4 μg/ml) or absence of Fab-B404 is shown. HSC-F cells were inoculated with undiluted SIVmac316 and NS, and 10-fold diluted NS. Viral infection was monitored 4 days post-infection using flow cytometry after intracellular staining by B450 (anti-p27 Fab). **(B)** Neutralization of SIVmac316 and NS by B404 in HSC-F cells are shown. Percent inhibition was calculated by comparison with the infected culture in the absence of B404.

increased infectivity for human cells. The premature stop codon in the gp41 cytoplasmic region was frequently detected in SIV strains propagated in human cell culture *in vitro*, such as the original SIVmac316 clone, SIVmac1A11 and 17E-Fr (Hirsch et al., 1989; Kodama et al., 1989; Mori et al., 1992; Bonavia et al., 2005; Vzorov et al., 2005). The truncation of gp41 is considered as an adaptation of SIV to replication in human cell culture, because the premature stop codon rapidly reverted to express full-length gp41 after infection of rhesus primary cell culture *in vitro* and rhesus macaques *in vivo* (Hirsch et al., 1989; Kodama et al., 1989). Mutant viruses harboring the gp41 truncation showed increased infectivity for human cells, although the effects on infectivity varied depending on the SIV strain and the length of the gp41 truncation (Manrique et al., 2001; Yuste et al., 2004, 2005; Vzorov et al., 2005, 2007). The enhancement effect of gp41 truncation on incorporation of Env into virions, which were demonstrated by quantification of viral proteins in virions (Yuste et al., 2004) and electron tomography analysis of Env trimers on virions (Zhu et al., 2003, 2006), was partly associated with the increased infectivity caused by gp41 truncation (Manrique et al., 2001; Yuste et al., 2004, 2005). Because expression of Env on the cell surface is regulated by the cytoplasmic domain of gp41, truncation of gp41 may increase Env density on both cells and virions (LaBranche et al., 1995; Berlioz-Torrent et al., 1999; Postler and Desrosiers, 2013). Consistent with these studies, infectivity for human cells and Env incorporation into virions was enhanced by gp41 truncation in the present study. Although the mechanism responsible for increasing viral infectivity caused by gp41 truncation remains unclear, the high virion Env content may contribute to the efficient replication of viruses with truncated gp41 in human cells.

The effect of gp41 truncation on susceptibility to antibody-mediated neutralization is controversial, perhaps due to the SIV strains used for the analyses. Because most of prototypic SIV clones with truncated gp41 were macrophage-tropic, CD4-independent, and neutralization-sensitive (Mori et al., 1992; Bonavia et al., 2005; Vzorov et al., 2005), the truncation of gp41 was assumed responsible for the high sensitivity to neutralization. However, the resistance to neutralization by gp41 truncation was shown using the E767stop mutant of SIVmac316 (Yuste et al., 2005). This is consistent with our results using SIVmac316 harboring the Q733stop substitution, indicating that gp41 truncation contributes to resistance of SIVmac316 to neutralization. The increased infectivity of viruses with gp41 truncation in human cells may partially play a role in resistance by overcoming antibody-mediated neutralization via efficient attachment and entry of viruses to cells. However, we showed that gp41 truncation was also associated with neutralization resistance in macaque cells, in which gp41 truncation did not significantly affect infectivity. This suggests that the increased infectivity in human cells does not significantly affect the neutralization resistance of viruses with truncated gp41. As shown by provision of excess Env in trans, high Env content in virions may be critical for antibody-mediated neutralization (Yuste et al., 2005). Further studies will be required to understand the mechanism of resistance to neutralization conferred by gp41 truncation.

In the present study, we demonstrated that truncation of the cytoplasmic tail of gp41 contributes to resistance to antibody-mediated neutralization. Although non-human primate models of SIV infection are commonly used to estimate vaccine efficacy, the lack of broadly neutralizing MAbs has hampered development of antibody-based vaccine candidates in an SIV-macaque model. The broadly neutralizing MAb B404, which neutralizes multiple, diverse SIV isolates (Kuwata et al., 2013), is a useful tool for understanding the mechanism of neutralization in an SIV-macaque model and will contribute to the development of HIV-1 vaccines.

ACKNOWLEDGMENTS

We thank Dr. Hirofumi Akari for providing HSC-F cells. TZM-bl cells were obtained from Dr. John C. Kappes, Dr. Xiaoyun Wu, and Tranzyme Inc. through the NIH AIDS Research and Reference Reagent Program, Division of AIDS, NIAID, NIH. This work

was supported by MEXT KAKENHI Grant Number 10839786, the Program of Founding Research Centres for Emerging and Re-emerging Infectious Diseases, the Global COE program Global Education and Research Centre Aiming at the Control of AIDS and a grant-in-aid for scientific research (C-24591484) from the Ministry of Education, Culture, Sport, Science and Technology, Japan and a grant from the Ministry of Health, Welfare and Labour of Japan (H24-AIDS-007).

REFERENCES

Akari, H., Nam, K. H., Mori, K., Otani, I., Shibata, H., Adachi, A., et al. (1999). Effects of SIVmac infection on peripheral blood CD4+CD8+ T lymphocytes in cynomolgus macaques. *Clin. Immunol.* 91, 321–329.

Berlioz-Torrent, C., Shacklett, B. L., Erdtmann, L., Delamarre, L., Bouchaert, I., Sonigo, P., et al. (1999). Interactions of the cytoplasmic domains of human and simian retroviral transmembrane proteins with components of the clathrin adaptor complexes modulate intracellular and cell surface expression of envelope glycoproteins. *J. Virol.* 73, 1350–1361.

Bonavia, A., Bullock, B. T., Gisselman, K. M., Margulies, B. J., and Clements, J. E. (2005). A single amino acid change and truncated TM are sufficient for simian immunodeficiency virus to enter cells using CCR5 in a CD4-independent pathway. *Virology* 341, 12–23.

Derdeyn, C. A., Decker, J. M., Sfakianos, J. N., Wu, X., O'Brien, W. A., Ratner, L., et al. (2000). Sensitivity of human immunodeficiency virus type 1 to the fusion inhibitor T-20 is modulated by coreceptor specificity defined by the V3 loop of gp120. *J. Virol.* 74, 8358–8367.

DuBridge, R. B., Tang, P., Hsia, H. C., Leong, P. M., Miller, J. H., and Calos, M. P. (1987). Analysis of mutation in human cells by using an Epstein–Barr virus shuttle system. *Mol. Cell. Biol.* 7, 379–387.

Hatada, M., Yoshimura, K., Harada, S., Kawanami, Y., Shibata, J., and Matsushita, S. (2010). Human immunodeficiency virus type 1 evasion of a neutralizing anti-V3 antibody involves acquisition of a potential glycosylation site in V2. *J. Gen. Virol.* 91, 1335–1345.

Haynes, B. F., Gilbert, P. B., Mcelrath, M. J., Zolla-Pazner, S., Tomaras, G. D., Alam, S. M., et al. (2012). Immune-correlates analysis of an HIV-1 vaccine efficacy trial. *N. Engl. J. Med.* 366, 1275–1286.

Hirsch, V. M., Edmondson, P., Murphey-Corb, M., Arbeille, B., Johnson, P. R., and Mullins, J. I. (1989). SIV adaptation to human cells. *Nature* 341, 573–574.

Kodama, T., Wooley, D. P., Naidu, Y. M., Kestler, H. W. III, Daniel, M. D., Li, Y., et al. (1989). Significance of premature stop codons in env of simian immunodeficiency virus. *J. Virol.* 63, 4709–4714.

Kuwata, T., Katsumata, Y., Takaki, K., Miura, T., and Igarashi, T. (2011). Isolation of potent neutralizing monoclonal antibodies from an SIV-Infected rhesus macaque by phage display. *AIDS Res. Hum. Retroviruses* 27, 487–500.

Kuwata, T., Takaki, K., Yoshimura, K., Enomoto, I., Wu, F., Ourmanov, I., et al. (2013). Conformational epitope consisting of the V3 and V4 loops as a target for potent and broad neutralization of simian immunodeficiency viruses. *J. Virol.* 87, 5424–5436.

Kwong, P. D., and Mascola, J. R. (2012). Human antibodies that neutralize HIV-1: identification, structures, and B cell ontogenies. *Immunity* 37, 412–425.

LaBranche, C. C., Sauter, M. M., Haggarty, B. S., Vance, P. J., Romano, J., Hart, T. K., et al. (1995). A single amino acid change in the cytoplasmic domain of the simian immunodeficiency virus transmembrane molecule increases envelope glycoprotein expression on infected cells. *J. Virol.* 69, 5217–5227.

Lusso, P., Cocchi, F., Balotta, C., Markham, P. D., Louie, A., Farci, P., et al. (1995). Growth of macrophagetropic and primary human immunodeficiency virus type 1 (HIV-1) isolates in a unique CD4+ T-cell clone (PM1): failure to downregulate CD4 and to interfere with cell-line-tropic HIV-1. *J. Virol.* 69, 3712–3720.

Manrique, J. M., Celma, C. C., Affranchino, J. L., Hunter, E., and Gonzalez, S. A. (2001). Small variations in the length of the cytoplasmic domain of the simian immunodeficiency virus transmembrane protein drastically affect envelope incorporation and virus entry. *AIDS Res. Hum. Retroviruses* 17, 1615–1624.

Matsumi, S., Matsushita, S., Yoshimura, K., Javaherian, K., and Takatsuki, K. (1995). Neutralizing monoclonal antibody against a external envelope glycoprotein (gp110) of SIVmac251. *AIDS Res. Hum. Retroviruses* 11, 501–508.

Mori, K., Ringler, D. J., Kodama, T., and Desrosiers, R. C. (1992). Complex determinants of macrophage tropism in env of simian immunodeficiency virus. *J. Virol.* 66, 2067–2075.

Platt, E. J., Wehrly, K., Kuhmann, S. E., Chesebro, B., and Kabat, D. (1998). Effects of CCR5 and CD4 cell surface concentrations on infections by macrophagetropic isolates of human immunodeficiency virus type 1. *J. Virol.* 72, 2855–2864.

Postler, T. S., and Desrosiers, R. C. (2013). The tale of the long tail: the cytoplasmic domain of HIV-1 gp41. *J. Virol.* 87, 2–15.

Reed, L. J., and Muench, H. (1938). A simple method of estimating fifty per cent endpoints. *Am. J. Epidemiol.* 27, 493–497.

Rerks-Ngarm, S., Pitisuttithum, P., Nitayaphan, S., Kaewkungwal, J., Chiu, J., Paris, R., et al. (2009). Vaccination with ALVAC and AIDSVAX to prevent HIV-1 infection in Thailand. *N. Engl. J. Med.* 361, 2209–2220.

Takeuchi, Y., Mcclure, M. O., and Pizzato, M. (2008). Identification of gammaretroviruses constitutively released from cell lines used for human immunodeficiency virus research. *J. Virol.* 82, 12585–12588.

Tamura, K., Peterson, D., Peterson, N., Stecher, G., Nei, M., and Kumar, S. (2011). MEGA5: molecular evolutionary genetics analysis using maximum likelihood, evolutionary distance, and maximum parsimony methods. *Mol. Biol. Evol.* 28, 2731–2739.

Vzorov, A. N., Gernert, K. M., and Compans, R. W. (2005). Multiple domains of the SIV Env protein determine virus replication efficiency and neutralization sensitivity. *Virology* 332, 89–101.

Vzorov, A. N., Weidmann, A., Kozyr, N. L., Khaoustov, V., Yoffe, B., and Compans, R. W. (2007). Role of the long cytoplasmic domain of the SIV Env glycoprotein in early and late stages of infection. *Retrovirology* 4, 94.

Wei, X., Decker, J. M., Liu, H., Zhang, Z., Arani, R. B., Kilby, J. M., et al. (2002). Emergence of resistant human immunodeficiency virus type 1 in patients receiving fusion inhibitor (T-20) monotherapy. *Antimicrob. Agents Chemother.* 46, 1896–1905.

Yoshimura, K., Shibata, J., Kimura, T., Honda, A., Maeda, Y., Koito, A., et al. (2006). Resistance profile of a neutralizing anti-HIV monoclonal antibody, KD-247, that shows favourable synergism with anti-CCR5 inhibitors. *AIDS* 20, 2065–2073.

Yusa, K., Maeda, Y., Fujioka, A., Monde, K., and Harada, S. (2005). Isolation of TAK-779-resistant HIV-1 from an R5 HIV-1 GP120 V3 loop library. *J. Biol. Chem.* 280, 30083–30090.

Yuste, E., Johnson, W., Pavlakis, G. N., and Desrosiers, R. C. (2005). Virion envelope content, infectivity, and neutralization sensitivity of simian immunodeficiency virus. *J. Virol.* 79, 12455–12463.

Yuste, E., Reeves, J. D., Doms, R. W., and Desrosiers, R. C. (2004). Modulation of Env content in virions of simian immunodeficiency virus: correlation with cell surface expression and virion infectivity. *J. Virol.* 78, 6775–6785.

Zhu, P., Chertova, E., Bess, J., Lifson, J. D., Arthur, L. O., Liu, J., et al. (2003). Electron tomography analysis of envelope glycoprotein trimers on HIV and simian immunodeficiency virus virions. *Proc. Natl. Acad. Sci. U.S.A.* 100, 15812–15817.

Zhu, P., Liu, J., Bess, J., Chertova, E., Lifson, J. D., Grisé, H., et al. (2006). Distribution and three-dimensional structure of AIDS virus envelope spikes. *Nature* 441, 847–852.

Conflict of Interest Statement: The authors declare that the research was conducted in the absence of any commercial or financial relationships that could be construed as a potential conflict of interest.

Received: 22 March 2013; accepted: 25 April 2013; published online: 14 May 2013.

Citation: Kuwata T, Takaki K, Enomoto I, Yoshimura K and Matsushita S (2013) Increased infectivity in human cells and resistance to antibody-mediated neutralization by truncation of the SIV gp41 cytoplasmic tail. Front. Microbiol. 4:117. doi: 10.3389/fmicb.2013.00117

This article was submitted to Frontiers in Virology, a specialty of Frontiers in Microbiology.

Bioorganic & Medicinal Chemistry Letters 20 (2010) 354–358

Contents lists available at ScienceDirect

Bioorganic & Medicinal Chemistry Letters

journal homepage: www.elsevier.com/locate/bmcl

CD4 mimics targeting the mechanism of HIV entry

Yuko Yamada [a], Chihiro Ochiai [a], Kazuhisa Yoshimura [b], Tomohiro Tanaka [a], Nami Ohashi [a], Tetsuo Narumi [a], Wataru Nomura [a], Shigeyoshi Harada [b], Shuzo Matsushita [b], Hirokazu Tamamura [a,*]

[a] Institute of Biomaterials and Bioengineering, Tokyo Medical and Dental University, Chiyoda-ku, Tokyo 101-0062, Japan
[b] Center for AIDS Research, Kumamoto University, Kumamoto 860-0811, Japan

ARTICLE INFO

Article history:
Received 19 September 2009
Revised 20 October 2009
Accepted 22 October 2009
Available online 4 November 2009

Keywords:
CD4 mimic
HIV entry
Synergistic effect
CXCR4

ABSTRACT

A structure–activity relationship study was conducted of several CD4 mimicking small molecules which block the interaction between HIV-1 gp120 and CD4. These CD4 mimics induce a conformational change in gp120, exposing its co-receptor-binding site. This induces a highly synergistic interaction in the use in combination with a co-receptor CXCR4 antagonist and reveals a pronounced effect on the dynamic supramolecular mechanism of HIV-1 entry.

Recently, remarkable success has attended the clinical treatment of HIV-infected and AIDS patients, with 'highly active antiretroviral therapy (HAART)'. This approach involves a combination of two or three agents from two categories: reverse transcriptase inhibitors and protease inhibitors.[1] In addition, the molecular mechanism involved in HIV-entry and -fusion into host cells has been described in detail.[2] The complex interactions of surface proteins on cellular and viral membranes, which are designated as a dynamic supramolecular mechanism of HIV entry, are reported to be crucial to the viral infection. In a first step, an HIV envelope protein, gp120 interacts with a cell surface protein, CD4, leading to a conformational change in gp120 followed by subsequent binding of gp120 to a co-receptor CCR5[3] or CXCR4.[4] CCR5 and CXCR4 are the major co-receptors for the entry of macrophage-tropic (R5-) and T cell line-tropic (X4-) HIV-1, respectively. The interaction of gp120 with CCR5 or CXCR4 triggers entry of another envelope protein, gp41 to the cell membrane and formation of a gp41 trimer-of-hairpins structure, which causes fusion of HIV/cell-membranes and completes the infection.

Informed by this mechanism, a fusion inhibitor, enfuvirtide (fuzeon, Trimers & Roche)[5] and a CCR5 antagonist, maraviroc (Pfizer)[6] in addition to an integrase inhibitor, raltegravir (Merck)[7] have been used clinically. However, serious problems with chemotherapy still persist, including the emergence of viral strains with multi-drug resistance (MDR), considerable adverse effects and high costs. Consequently, development of novel drugs possessing mechanisms of action different from those of the above inhibitors is currently required. We have previously developed selective CXCR4 antagonists[8] and fusion inhibitors.[9] Furthermore, *N*-(4-Bromophenyl)-*N'*-(2,2,6,6-tetramethylpiperidin-4-yl)-oxalamide (**1**) and *N*-(4-chlorophenyl)-*N'*-(2,2,6,6-tetramethylpiperidin-4-yl)-oxalamide (**2**) were previously found using chemical library screening to inhibit syncytium formation by other researchers.[10] **1** and **2** bind to gp120 with binding affinities of K_d = 2.2 μM and 3.7 μM, respectively, blocking the interaction of gp120 with CD4 in the first step of an HIV-1 entry. Thus, in the present study we focus on the development of CD4 mimics that can block the interaction between gp120 and CD4. We have investigated the effect of CD4 mimics on conformational changes of gp120 and on their use in combination use with a CXCR4 antagonist.

Initially, molecular modeling of compound **2** docked into gp120 was carried out using docking simulations performed by the FlexSIS module of SYBYL 7.1 (Tripos, St. Louis) (Fig. 1).[11] The atomic coordinates of the crystal structure of gp120 with soluble CD4 (sCD4) were retrieved from Protein Data Bank (PDB) (entry 1RZJ) (Fig. 1a) and it was observed that Phe^{43} and Arg^{59} of the CD4 have multiple contacts with Asp^{368}, Glu^{370} and Trp^{427} of gp120, which are all conserved residues. An inspection of the environment of compound **2** docked in gp120 revealed the presence of a large cavity around the *p*-position of the phenyl ring of compound **2**, which could interact with the viral surface protein gp120 (Fig. 1b and c). Several analogs of **2** with substituents on the phenyl ring were therefore synthesized.

All compounds except **12** were synthesized by previously published methods (Scheme 1).[10b,12,13] Aniline derivatives (**3**) were coupled with ethyl oxalyl chloride to yield the corresponding ethyl oxalamates **4**. Saponification of the above oxalamates to the corresponding free acids and the subsequent coupling with 4-ami-

* Corresponding author.
E-mail address: tamamura.mr@tmd.ac.jp (H. Tamamura).

0960-894X/$ - see front matter © 2009 Elsevier Ltd. All rights reserved.
doi:10.1016/j.bmcl.2009.10.098

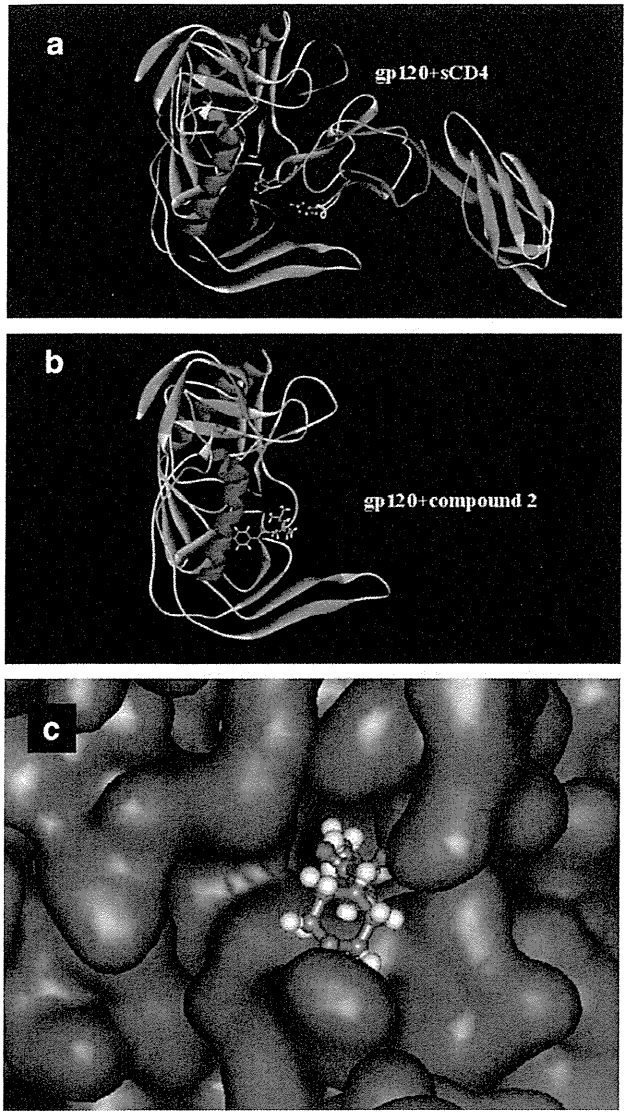

Figure 1. (a) The crystal structure of gp120 with soluble CD4 (sCD4) retrieved from the PDB (entry 1RZJ); (b) docking structure of compound **2** and gp120; (c) a focused figure of (b) shown by space-filling model.

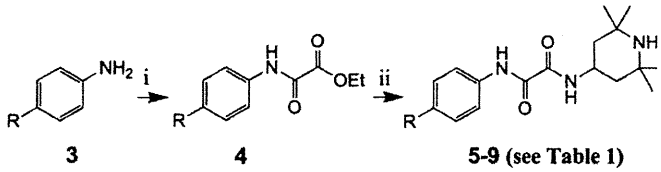

Scheme 1. Reagents and conditions: (i) ethyl oxalyl chloride, Et_3N; (ii) 1 M NaOH; 4-amino-2,2,6,6-tetramethylpiperidine, 1-(3-dimethylaminopropyl)-3-ethylcarbodiimide hydrochloride, 1-hydroxybenzotriazole, Et_3N.

no-2,2,6,6-tetramethylpiperidine using 1-ethyl-3-(3-dimethylaminopropyl)carbodiimide hydrochloride (EDC) and 1-hydroxybenzotriazole (HOBt) yielded compounds **5–9**. In the case of compound **12**, whose amide bond is not stable during the reaction of the saponification of the corresponding oxalamates, an alternative synthetic scheme was used (Scheme 2).[14] The reaction of *p*-nitroaniline (**10**) with oxalyl chloride gave the corresponding oxoacetamide **11**, which was subsequently coupled with 4-amino-2,2,6,6-tetramethylpiperidine to yield the desired compound **12**.

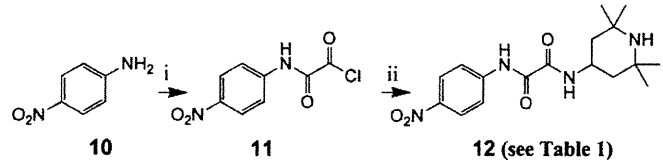

Scheme 2. Reagents and conditions: (i) oxalyl chloride, Et_3N; (ii) 4-amino-2,2,6,6-tetramethylpiperidine, Et_3N.

The anti-HIV activity of the synthetic compounds was evaluated against various viral strains including both laboratory and primary isolates (Table 1). IC_{50} values were determined by the 3-(4,5-dimethylthiazol-2-yl)-2,5-diphenyltetrazolium bromide (MTT) method[15] as the concentrations of the compounds which conferred 50% protection against HIV-1-induced cytopathogenicity in PM1/CCR5 cells. Cytotoxicity of the compounds based on the viability of mock-infected PM1/CCR5 cells was also evaluated using the MTT method. CC_{50} values were determined as the concentrations achieving 50% reduction of the viability of mock-infected cells. Compounds **1** and **2** showed potent anti-HIV activity against laboratory isolates, IIIB (X4, Sub B) and 89.6 (dual, Sub B) strains, and compound **2** also possessed potent activity against a primary isolate, an fTOI strain (R5, Sub B). All of the IC_{50} values were between 4 μM and 10 μM. Compound **1** was not tested against primary isolates. The potencies of compounds **1** and **2** are comparable to the reported binding affinities for gp120 (K_d = 2.2 and 3.7 μM, respectively).[10] Several of the new analogs of compounds **1** and **2** showed significant anti-HIV activity. Compound **5**, which has a phenyl group in place of the *p*-chlorophenyl group of compound **2**, did not show significant anti-HIV activity at concentrations below 100 μM against all strains tested except for an fTOI strain (R5, Sub B). This result suggests that a substituent at the *p*-position of the phenyl ring is critical for potent activity. Compound **6**, which has a fluorine atom at the *p*-position of the phenyl ring, showed moderate anti-HIV activity against laboratory isolates, IIIB (X4, Sub B) and 89.6 (dual, Sub B) strains (IC_{50} = 61 and 81 μM, respectively), but, at concentrations below 100 μM, failed to show significant anti-HIV activity against a primary isolate, a KYAG strain (R5, Sub B). Among halogen atoms, fluorine is less suitable than bromine or chlorine as a substituent at the *p*-position of the phenyl ring, as evidenced by compound **6**, which is 8–15-fold less potent than compounds **1** and **2** against IIIB (X4, Sub B) and 89.6 (dual, Sub B) strains. Compound **7**, which has a methyl group at the *p*-position of the phenyl ring, showed relatively more potent activity against IIIB (X4, Sub B) and 89.6 (dual, Sub B) strains (IC_{50} = 23 and 41 μM, respectively) than compound **6**. Compound **7** also showed significant anti-HIV activity against primary isolates, fTOI (R5, Sub B) and KYAG (R5, Sub B) strains (IC_{50} = 16 and 51 μM, respectively). Compound **8**, with a methoxy group at the *p*-position of the phenyl ring, did not show significant anti-HIV activity against all strains tested until a concentration of 100 μM was reached. In the biological assays, derivatives having electron-withdrawing substituents such as bromine, chlorine and fluorine at the *p*-position of the phenyl ring are relatively potent, whereas derivatives having electron-donating groups such as methoxy at this position are not potent. Furthermore, the steric effect of a substituent at the *p*-position of the phenyl ring appears to be critical to anti-HIV activity. The sum of Hammett constants (σ) of benzoic acid substituents[16] shown in Table 1 can be used to evaluate the electron-withdrawing or -donating effect of the substituents on the aromatic ring. The Taft E_s values[16a,17] were used as steric parameters for substituents at the *p*-position of the phenyl ring. The order of potency found for the halogen-containing derivatives in anti-HIV activity against laboratory isolates, IIIB (X4, Sub B) and 89.6 (dual, Sub B), is: compound **1** (R = Br) (σ = 0.23, E_s = −1.16), **2**

Table 1
Hammett constants (σ) and steric effects (E_s) of substituted aromatic rings and anti-HIV activity and cytotoxicity of synthetic compounds

Compd	R[a]	σ[b]	E_s[c]	IC_{50}[e] (μM)				CC_{50}[e] (μM)
				Lab. isolates		Primary isolates		
				IIIB (X4)	89.6 (dual)	fTOI (R5)	KYAG (R5)	
1	Br	0.23	−1.16	4	9	ND	ND	150
2	Cl	0.23	−0.97	8	10	5	>30	170
5	H	0	0	>100	>100	81	>100	350
6	F	0.06	−0.46	61	81	ND	>100	320
7	CH_3	−0.17	−1.24	23	41	16	51	210
8	OCH_3	−0.27	−0.55	>100	>100	ND	>100	340
9	CF_3	0.54	−2.40	ND	27	ND	ND	72
12	NO_2	0.78	−1.77[d]	ND	42	ND	ND	230
sCD4				0.010	0.021	0.0044	ND	ND

[a] See Schemes 1 and 2.
[b] σ = Hammett constant of a substitutent on a benzoic acid derivative.[16]
[c] E_s = steric effect of a substituent at the *para* position on the aromatic ring.[16a,17]
[d] The average value of −1.01 and −2.52, which are E_s values of the NO_2 group, −1.77, was used.
[e] Values are means of at least three experiments (ND = not determined).

(R = Cl) (σ = 0.23, E_s = −0.97), **6** (R = F) (σ = 0.06, E_s = −0.46) and **5** (R = H) (σ = 0, E_s = 0). This is the order of substituents' electron-withdrawing ability and also of their size. Methyl (σ = −0.17, E_s = −1.24) is an electron-donating group, but is almost as bulky as a bromine atom. Thus, the *p*-methyl derivative **7** has relatively potent anti-HIV activity against laboratory isolates, IIIB (X4, Sub B) and 89.6 (dual, Sub B), higher than that of compound **6** (R = F) but lower than that of compound **1** (R = Br) or **2** (R = Cl). The electron-donating ability of a methoxy group is stronger (σ = −0.27), but the bulk size is smaller (E_s = −0.55), than that of a methyl group. Thus, the *p*-methoxy derivative **8** has no significant anti-HIV activity against all strains tested at concentrations below 100 μM. Two derivatives containing bulkier and more potent electron-withdrawing substituents such as trifluoromethyl (R = CF_3) (σ = 0.54, E_s = −2.40) and nitro (R = NO_2) (σ = 0.78, E_s = −1.77) at the *p*-position of the phenyl ring were evaluated. Compounds **9** (R = CF_3) and **12** (R = NO_2) showed significant anti-HIV activity against an 89.6 (dual, Sub B) strain. These are less potent than compounds **1** and **2** and this is perhaps due to the excessive size of the substituents at the *p*-position. This suggests that a certain level of the bulk size and a potent electron-withdrawing ability of the substituents are preferable for anti-HIV activity. It is estimated that a cavity around the *p*-position of the phenyl ring of CD4 mimicking compounds would be optimally filled by bromine (E_s = −1.16) or a methyl group (E_s = −1.24) at *p*-position, and that an electron-deficient aromatic ring might interact tightly with a negatively charged group such as carboxy of Glu^{370}. In isothermal titration calorimetry (ITC) experiments reported elsewhere,[10c] compound **5** (R = H) does not have significant affinity for gp120, and compound **6** (R = F) has less potent affinity for gp120 than compound **2**, consistent with the present data. In all but one of the compounds, no significant cytotoxicity was detected (CC_{50} >150 μM, Table 1), the exception being compound **9** (R = CF_3) (CC_{50} = 72 μM). Compounds **7** and **12** have relatively low cytotoxicities, compared to compounds **1** and **2**.

Fluorescence activated cell sorting (FACS) analysis was performed[15] to investigate whether these synthetic compounds interact with gp120 inducing the conformational change necessary for the approach of an anti-envelope antibody or a co-receptor to the gp120. The profile of binding of an anti-envelope CD4-induced monoclonal antibody, 4C11, to the Env-expressing cell surface (an R5-HIV-1 strain, JR-FL,-infected PM1 cells) pretreated with the above CD4 mimic analogs was examined. Comparison of the binding of 4C11 to the cell surface was measured in terms of the mean fluorescence intensity (MFI), and is shown in Figure 2. Pretreatment of the Env-expressing cells with compound **2** (MFI = 38.42) produced a remarkable increase in binding affinity for 4C11, similar to that observed in pretreatment with sCD4 (MFI = 37.90). This is consistent with the results in the previous paper[10] where it was reported that compound **2** enhances the binding of gp120 to the 17b monoclonal antibody which recognizes the co-receptor binding site of gp120. Env-expressing cells, which were not pretreated with sCD4 or a CD4 mimic compound, did not show significant binding affinity for 4C11 (Fig. 2, blank). The increase in binding affinity for monoclonal antibodies may be due to conformational changes in gp120, which were caused by the interaction of sCD4 or a CD4 mimic with gp120. It is hypothesized that such conformational changes involve the exposure of the co-receptor binding site of gp120 (the V3 loop), which is hidden internally, since the binding of gp120 to 17b is enhanced. Compound **5**, which failed to show significant anti-HIV activity, and compounds **7**, **9** and **12**, which had significant anti-HIV activity, were assessed in the FACS analysis. The profile of the binding of 4C11 to the Env-expressing cell surface pretreated with compound **5** (MFI = 14.34) was similar to that of the blank (MFI = 11.24), suggesting that compound **5** offers no significant enhancement of binding affinity for 4C11. This result is compatible with the anti-HIV activity of compound **5**. The profile of the binding of 4C11 to the Env-expressing cell surface pretreated with compound **7** (MFI = 38.33) was entirely similar to that of compound **2** used as a pretreatment. Pretreatment of the cell surface with compounds **9** and **12** (MFI = 29.09 and 30.01, respectively) produced a slightly lower enhancement of binding affinity for 4C11, compared to those of compounds **2** and **7** as pretreatments. However, in the ITC experiments reported elsewhere,[10c] compound **9** (R = CF_3) has a high affinity for gp120, comparable to that of compound **2**, but compound **12** (R = NO_2) does not have significant affinity for gp120, indicating that these are not consistent with the current FACS studies, possibly due to the difference in the assay systems. Although the anti-HIV activity of **7** is weaker than that of compound **2**, the level of compound **7** inducing an enhancement of binding affinity of gp120 for 4C11 is comparable to that of compound **2**. The concentration of compounds used in the FACS analysis was 100 μM, much beyond the IC_{50} values of compounds **2** and **7**. A concentration of 100 μM would be also sufficient for the expression of anti-HIV activity caused by compounds **2** and **7**.

An effect on the use of compound **2** combined with another entry inhibitor was investigated. Analysis of the synergistic effects of anti-HIV agents was performed according to the median effect principle using the CalcuSyn version 2 computer program[18] to estimate IC_{50} values of compounds in different combinations. Combination indices (CI) were estimated from the data evaluated using the MTT assay

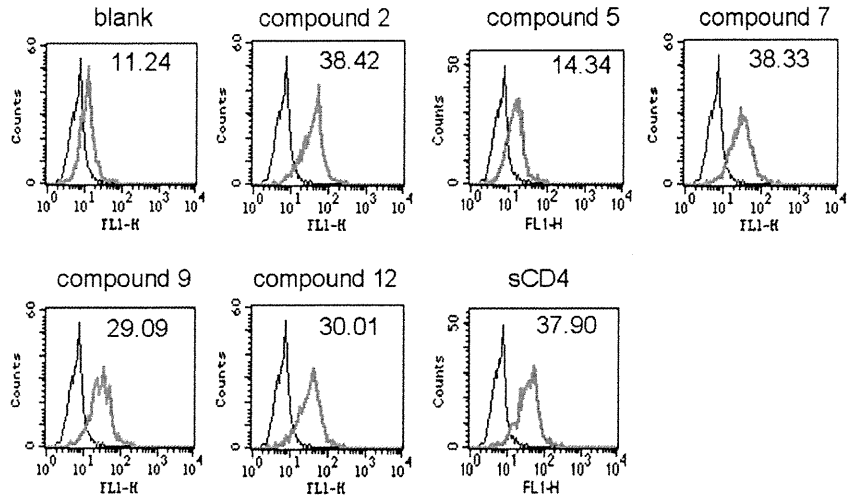

Figure 2. JR-FL (R5, Sub B) chronically infected PM1 cells were preincubated with 100 μM of a CD4 mimic or sCD4 (11 nM) for 15 min, and then incubated with an anti-HIV-1 mAb, 4C11, at 4 °C for 15 min. The cells were washed with PBS, and fluorescein isothiocyanate (FITC)-conjugated goat anti-human IgG antibody was used for antibody-staining. Flow cytometry data for the binding of 4C11 (green lines) to the Env-expressing cell surface in the presence of sCD4 or a CD4 mimic are shown among gated PM1 cells along with a control antibody (anti-human CD19: black lines). Data are representative of the results from a minimum of two independent experiments. The number at the top of each graph shows the mean fluorescence intensity (MFI) of the antibody 4C11.

Table 2
Combination indices (CI) for compound **2** or sCD4 and a CXCR4 antagonist, T140, against an HIV IIIB strain

Combination	HIV strain	CI values at different IC[a]		
		IC_{50}	IC_{75}	IC_{90}
2 + T140	IIIB	0.786	0.713	0.655
sCD4 + T140	IIIB	0.705	0.528	0.400

[a] The multiple-drug effect analysis reported by Chou et al. was used to analyze the effects of combinational uses of compounds.[18] CI <0.9: synergy, 0.9 < CI < 1.1: additivity, CI >1.1: antagonism.

(Table 2).[15] Compound **2** showed a highly remarkable synergistic anti-HIV activity with a co-receptor CXCR4 antagonist, T140,[8a] against an X4-HIV-1 strain, IIIB at various IC values (IC_{50}, IC_{75} and IC_{90}). However, sCD4 exhibited a higher synergistic effect (lower CI values) with T140 (Table 2). The interaction of sCD4 or a CD4 mimic with gp120 would expose the co-receptor-binding site of gp120, and the co-receptor CXCR4 could then easily approach gp120. Thus, an inhibitory effect of a CXCR4 antagonist would be meaningful, and a significant synergistic effect might also be brought about by a combination of sCD4 or a CD4 mimic and T140.

In summary, a series of CD4 mimic compounds were synthesized and evaluated for their anti-HIV activity. Several compounds showed significant anti-HIV activity with relatively low cytotoxicity. SAR studies showed that a certain level of size and electron-withdrawing ability of the substituents at the *p*-position of the phenyl ring are suitable for potent anti-HIV activity. In addition, the treatment of Env-expressing cells with several CD4 mimicking compounds causes a conformational change, exposing the co-receptor-binding site of gp120 externally. Thus, a CD4 mimic exhibited a remarkable synergistic effect with a co-receptor antagonist. These compounds are essential probes directed to the dynamic supramolecular mechanism of HIV entry, and important leads for the cocktail therapy of AIDS.

Acknowledgments

This work was supported by Mitsui Life Social Welfare Foundation, Grant-in-Aid for Scientific Research from the Ministry of Education, Culture, Sports, Science, and Technology of Japan, and Health and Labour Sciences Research Grants from Japanese Ministry of Health, Labor, and Welfare.

References and notes

1. Mitsuya, H.; Erickson, J. In *Textbook of AIDS Medicine*; Merigan, T. C., Bartlett, J. G., Bolognesi, D., Eds.; Williams & Wilkins: Baltimore, 1999; pp 751–780.
2. Chan, D. C.; Kim, P. S. *Cell* **1998**, *93*, 681.
3. (a) Alkhatib, G.; Combadiere, C.; Broder, C. C.; Feng, Y.; Kennedy, P. E.; Murphy, P. M.; Berger, E. A. *Science* **1996**, *272*, 1955; (b) Choe, H.; Farzan, M.; Sun, Y.; Sullivan, N.; Rollins, B.; Ponath, P. D.; Wu, L.; Mackay, C. R.; LaRosa, G.; Newman, W.; Gerard, N.; Gerard, C.; Sodroski, J. *Cell* **1996**, *85*, 1135; (c) Deng, H. K.; Liu, R.; Ellmeier, W.; Choe, S.; Unutmaz, D.; Burkhart, M.; Marzio, P. D.; Marmon, S.; Sutton, R. E.; Hill, C. M.; Davis, C. B.; Peiper, S. C.; Schall, T. J.; Littman, D. R.; Landau, N. R. *Nature* **1996**, *381*, 661; (d) Doranz, B. J.; Rucker, J.; Yi, Y. J.; Smyth, R. J.; Samson, M.; Peiper, S. C.; Parmentier, M.; Collman, R. G.; Doms, R. W. *Cell* **1996**, *85*, 1149; (e) Dragic, T.; Litwin, V.; Allaway, G. P.; Martin, S. R.; Huang, Y.; Nagashima, K. A.; Cayanan, C.; Maddon, P. J.; Koup, R. A.; Moore, J. P.; Paxton, W. A. *Nature* **1996**, *381*, 667.
4. Feng, Y.; Broder, C. C.; Kennedy, P. E.; Berger, E. A. *Science* **1996**, *272*, 872.
5. Wild, C. T.; Greenwell, T. K.; Matthews, T. J. *AIDS Res. Hum. Retroviruses* **1993**, *9*, 1051.
6. (a) Dorr, P.; Westby, M.; Dobbs, S.; Griffin, P.; Irvine, B.; Macartney, M.; Mori, J.; Rickett, G.; Smith-Burchnell, C.; Napier, C.; Webster, R.; Armour, D.; Price, D.; Stammen, B.; Wood, A.; Perros, M. *Antimicrob. Agents Chemother.* **2005**, *49*, 4721; (b) Price, D. A.; Armour, D.; De Groot, M.; Leishman, D.; Napier, C.; Perros, M.; Stammen, B. L.; Wood, A. *Bioorg. Med. Chem. Lett.* **2006**, *16*, 4633.
7. (a) Cahn, P.; Sued, O. *Lancet* **2007**, *369*, 1235; (b) Grinsztejn, B.; Nguyen, B.-Y.; Katlama, C.; Gatell, J. M.; Lazzarin, A.; Vittecoq, D.; Gonzalez, C. J.; Chen, J.; Harvey, C. M.; Isaacs, R. D. *Lancet* **2007**, *369*, 1261.
8. (a) Tamamura, H.; Xu, Y.; Hattori, T.; Zhang, X.; Arakaki, R.; Kanbara, K.; Omagari, A.; Otaka, A.; Ibuka, T.; Yamamoto, N.; Nakashima, H.; Fujii, N. *Biochem. Biophys. Res. Commun.* **1998**, *253*, 877; (b) Fujii, N.; Oishi, S.; Hiramatsu, K.; Araki, T.; Ueda, S.; Tamamura, H.; Otaka, A.; Kusano, S.; Terakubo, S.; Nakashima, H.; Broach, J. A.; Trent, J. O.; Wang, Z.; Peiper, S. C. *Angew. Chem., Int. Ed.* **2003**, *42*, 3251; (c) Tanaka, T.; Nomura, W.; Narumi, T.; Esaka, A.; Oishi, S.; Ohashi, N.; Itotani, K.; Evans, B. J.; Wang, Z.; Peiper, S. C.; Fujii, N.; Tamamura, H. *Org. Biomol. Chem.* **2009**, *7*, 3805.
9. Otaka, A.; Nakamura, M.; Nameki, D.; Kodama, E.; Uchiyama, S.; Nakamura, S.; Nakano, H.; Tamamura, H.; Kobayashi, Y.; Matsuoka, M.; Fujii, N. *Angew. Chem., Int. Ed.* **2002**, *41*, 2937.
10. (a) Zhao, Q.; Ma, L.; Jiang, S.; Lu, H.; Liu, S.; He, Y.; Strick, N.; Neamati, N.; Debnath, A. K. *Virology* **2005**, *339*, 213; (b) Schön, A.; Madani, N.; Klein, J. C.; Hubicki, A.; Ng, D.; Yang, X.; Smith, A. B., III; Sodroski, J.; Freire, E. *Biochemistry* **2006**, *45*, 10973; (c) Madani, N.; Schön, A.; Princiotto, A. M.; LaLonde, J. M.; Courter, J. R.; Soeta, T.; Ng, D.; Wang, L.; Brower, E. T.; Xiang, S.-H.; Do Kwon, Y.; Huang, C.-C.; Wyatt, R.; Kwong, P. D.; Freire, E.; Smith, A. B., III; Sodroski, J. *Structure* **2008**, *16*, 1689; (d) Haim, H.; Si, Z.; Madani, N.; Wang, L.; Courter, J. R.; Princiotto, A.; Kassa, A.; DeGrace, M.; McGee-Estrada, K.; Mefford, M.; Gabuzda, D.; Smith, A. B., III; Sodroski, J. *ProS Pathogens* **2009**, *5*, 1.
11. The structure of compound **2** was built in Sybyl and minimized with the MMFF94 force field and partial charges. (see: Halgren, T. A. *J. Comput. Chem.* **1996**, *17*, 490.) Docking was then performed using FlexSIS through its SYBYL

module, into the crystal structure of gp120 (PDB, entry 1RZJ). The binding site was defined as residues Val^{255}, Asp^{368}, Glu^{370}, Ser^{375}, Ile^{424}, Trp^{427}, Val^{430} and Val^{475}, and included residues located within a radius 4.4 Å. The ligand was considered to be flexible, and all other options were set to their default values. Figures were generated with ViewerLite version 5.0 (Accelrys Inc., San Diego, CA).

12. *For example, the synthesis of compound* **7**: To a solution of ethyl oxalyl chloride (0.400 mL, 3.48 mmol) in THF (20 mL) were added triethylamine (Et_3N) (0.480 mL, 3.48 mmol) and *p*-toluidine (373 mg, 3.48 mmol) with stirring at 0 °C. The reaction mixture was allowed to warm to room temperature, and then stirred for 6 h. After removal by filtration of the resulting salts, the filtrate was concentrated under reduced pressure. The residue was extracted with EtOAc (50 mL), and the extract was washed successively with brine (20 mL), 1 M HCl (20 mL × 2), brine (20 mL), saturated $NaHCO_3$ (20 mL × 2) and brine (20 mL × 3), then dried over $MgSO_4$. Concentration under reduced pressure gave the crude ethyl oxalamate, which was used without further purification. To a solution of the crude ethyl oxalamate (640 mg, 3.09 mmol) in THF (30 mL) were added aqueous 1 M NaOH (3.40 mL, 3.40 mmol), water (50 mL) and MeOH (20 mL) with stirring at 0 °C. The reaction mixture was allowed to warm to room temperature, and then stirred for 20 h. After the addition of aqueous 1 M HCl (5 mL), MeOH and THF were evaporated under reduced pressure. The residue was acidified to pH 2 with 1 M HCl, and extracted with EtOAc (50 mL × 2). The combined organic layer was washed with brine (20 mL × 3), and dried over $MgSO_4$. Concentration under reduced pressure gave the crude acid, which was used for the next reaction without further purification. To a solution of the above crude acid (514 mg, 2.87 mmol) in THF (10 mL) were added 1-hydoxybenzotriazole (484 mg, 3.16 mmol), 4-amino-2,2,6,6-tetramethylpiperidine (446 μL, 2.58 mmol), 1-ethyl-3-(3-dimethylaminopropyl)carbodiimide hydrochloride (606 mg, 3.16 mmol) and Et_3N (0.439 mL, 3.16 mmol) with stirring at 0 °C. The reaction mixture was allowed to warm to room temperature, and then stirred for 20 h. After evaporation of THF, the residue was dissolved in $CHCl_3$ (50 mL). The mixture was washed with saturated $NaHCO_3$ (20 mL × 2) and brine (20 mL × 3), and dried over $MgSO_4$. Concentration under reduced pressure gave the crude crystalline mass. The usual work-up followed by recrystallization from EtOAc–*n*-hexane gave the title compound **7** (363 mg, 1.14 mmol, 39.8%) as colorless crystals, mp = 176 °C; δ_H (400 MHz; $CDCl_3$) 1.07 (1H, m, NH), 1.16 (6H, s, CH_3), 1.29 (6H, s, CH_3), 1.44 (2H, m, CH_2), 1.91 (1H, d, *J* 3.7, *CH*H), 1.94 (1H, d, *J* 3.7, CH*H*), 2.34 (3H, s, CH_3), 4.25 (1H, m, CH), 7.17 (2H, d, *J* 8.3, ArH), 7.33 (1H, m, NH), 7.50 (2H, d, *J* 8.4, ArH), 9.18 (1H, s, NH); HRMS (FAB), *m*/*z* calcd for $C_{18}H_{28}N_3O_2$ $(MH)^+$ 318.2182, found 318.2173.
13. McFarland, C.; Vicic, D. A.; Debnath, A. K. *Synthesis* **2006**, 807.
14. *The synthesis of compound* **12**: To a solution of Et_3N (417 μL, 3.00 mmol) and 4-nitroaniline (138 mg, 1.00 mmol) in THF (1.3 mL) was added oxalyl dichloride (85.8 μL, 1.00 mmol) with stirring at 0 °C. After being stirred for 30 min at 0 °C, Et_3N (167 μL, 1.20 mmol) and 4-amino-2,2,6,6-tetramethylpiperidine (156 μL, 0.90 mmol) were added. The reaction mixture was stirred for 6 h at 0 °C. After removal by filtration of the resulting salts, the filtrate was concentrated under reduced pressure. The residue was dissolved in $CHCl_3$ (20 mL), and the mixture was washed successively with brine (10 mL), saturated $NaHCO_3$ (10 mL × 2) and brine (10 mL × 3), and dried over $MgSO_4$. Concentration under reduced pressure followed by flash chromatography over silica gel with $CHCl_3$–MeOH (9:1) gave 42.4 mg (0.122 mmol, 13.5%) of the title compound **12** as colorless crystals, mp = 190 °C; δ_H (400 MHz; $CDCl_3$) 1.09 (1H, m, NH), 1.17 (6H, s, CH_3), 1.29 (6H, s, CH_3), 1.43 (2H, m, CH_2), 1.92 (1H, d, *J* 3.8, *CH*H), 1.95 (1H, d, *J* 3.8, CH*H*), 4.28 (1H, m, CH), 7.29 (1H, m, NH), 7.82 (2H, d, *J* 9.1, ArH), 8.28 (2H, d, *J* 9.1, ArH), 9.55 (1H, s, NH); HRMS (FAB), *m*/*z* calcd for $C_{17}H_{25}N_4O_4$ $(MH)^+$ 349.1876, found 349.1871.
15. Yoshimura, K.; Shibata, J.; Kimura, T.; Honda, A.; Maeda, Y.; Koito, A.; Murakami, T.; Mitsuya, H.; Matsushita, S. *AIDS* **2006**, *20*, 2065.
16. (a) Chapman, N. B.; Shorter, J. *Advances in Linear Free Energy Relationship*; Plenum Press: London, 1972; (b) Chapman, N. B.; Shorter, J. *Correlation Analysis in Chemistry*; Plenum Press: London, 1978; (c) Hansch, C.; Leo, A. J.; Hoekman, D. *Exploring QSAR, Hydrophobic, Electronic, and Steric Constants*; American Chemical Society: Washington, DC, 1995.
17. Taft, R. W. In *Steric Effects in Organic Chemistry*; Newman, M. S., Ed.; John Wiley: New York, 1956; p 556.
18. (a) Chou, T. C.; Talalay, P. *J. Biol. Chem.* **1977**, *252*, 6438; (b) Chou, T. C.; Hayball, M. P. *CalcuSyn*, 2nd ed.; Biosoft: Cambridge, UK, 1996.

Remodeling of Dynamic Structures of HIV-1 Envelope Proteins Leads to Synthetic Antigen Molecules Inducing Neutralizing Antibodies

Toru Nakahara,[†] Wataru Nomura,*[,†] Kenji Ohba,[‡] Aki Ohya,[†] Tomohiro Tanaka,[†] Chie Hashimoto,[†] Tetsuo Narumi,[†] Tsutomu Murakami,[‡] Naoki Yamamoto,[‡] and Hirokazu Tamamura*[,†]

Department of Medicinal Chemistry, Institute of Biomaterials and Bioengineering, Tokyo Medical and Dental University, 2-3-10 Kandasurugadai, Chiyoda-ku, Tokyo 101-0062, Japan, and AIDS Research Center, National Institute of Infectious Diseases, 1-23-1 Toyama, Shinjuku-ku, Tokyo 162-8640, Japan. Received November 16, 2009; Revised Manuscript Received February 28, 2010

A synthetic antigen targeting membrane-fusion mechanism of HIV-1 has a newly designed template with C3-symmetric linkers mimicking N36 trimeric form. The antiserum produced by immunization of the N36 trimeric form antigen showed structural preference in binding to N36 trimer and stronger inhibitory activity against HIV-1 infection than the N36 monomer. Our results suggest an effective strategy of HIV vaccine design based on a relationship to the native structure of proteins involved in HIV fusion mechanisms.

INTRODUCTION

Antibody-based therapy is one of the promising treatments for AIDS. In recent years, AIDS antibodies have been produced by immunization (*1*) and by de novo engineering of monoclonal antibodies (mAb) with molecular evolution tactics such as phage display (*2*). Despite enormous efforts, however, only a limited number of highly and broadly HIV-neutralizing human mAbs have been isolated and characterized. These antibodies include gp41 Abs, 2F5 (*3*−*6*) and 4E10 (*5*−*7*), and gp120 Abs, 2G12 (*8*) and b12 (*9*). gp41 is a transmembrane envelope glycoprotein, which is divided into an endodomain and an ectodomain by the transmembrane region; the latter contains a hydrophobic amino-terminal fusion peptide, followed by amino-terminal and carboxy-terminal leucine/isoleucine heptad repeat domains with helical structures (HR1 and HR2, respectively). In the membrane fusion process of HIV-1, these subunits form a "pre-bundle" complex. The HR1 and HR2 regions are termed the N-terminal helix (N36) and C-terminal helix (C34), respectively. These helices form a six-helical bundle consisting of a central parallel trimeric coiled-coil of N36 surrounded by C34 in an antiparallel hairpin fashion. In design of immunogens that elicit broadly neutralizing antibodies, a useful strategy is to produce molecules that mimic the natural trimer on the virion surface. Previous studies show that these molecules could be proteins expressed as a recombinant form or on the surface of particles such as pseudovirions or proteoliposomes (*10*−*12*). The X-ray crystallographic study of gp41 shows that the distances between any two residues at the N-terminus of N-region are almost equal at approximately 10 Å (Figure 1A). A chemically synthetic template could be useful in connection with the design of a peptidomimetic corresponding to the native structure of gp41. To date, several gp41 mimetics have been synthesized as inhibitors or antigens and subjected to inhibition or neutralization assays (*13*−*16*). However, the templates for assembly of these helical peptides contain branched peptide linkers, which are not exactly equivalent in length (*14*). The N-terminal peptides constrained by another threefold linker showed high affinity for C-terminal peptides, although its biological advantages have not been determined (*15*). The mimicry can be estimated using the broadly neutralizing mAbs; suitable mimetics will bind neutralizing mAbs efficiently, but they will bind non-neutralizing mAbs poorly. In the present study, we designed and synthesized a novel three-helical bundle mimetic, which corresponds to the trimeric form of N36. We investigated whether mice immunized with the equivalent trimeric form of N36 mimetic can produce antibodies with stronger binding affinity for N36 trimer than for N36 monomer. This approach demonstrates the possibility of producing structure-specific antibodies by immunization of synthetic antigens corresponding to the natural form of viral proteins.

EXPERIMENTAL PROCEDURES

Conjugation of N36REGC and the Template to Produce triN36e. Compound **6** (100 μg, 0.174 μmol) and N36REGC (3.4 mg, 0.574 μmol) were dissolved in a mixture of 300 μL of 200 mM acetate buffer (pH 5.2) and 300 μL of TFE under a nitrogen atmosphere, then TCEP·HCl was added. The reaction was stirred for 72 h at room temperature and monitored by HPLC. The ligation product (triN36e) was separated as an HPLC peak and was characterized by ESI-TOF-MS, *m/z* calcd for $C_{690}H_{1160}N_{226}O_{201}S_3$ 15933.1, found 15933.8. The purification was performed by reverse phase HPLC (YMC-Pack ODS-A column, 10 × 250 mm). Elution was carried out with a 40−50% linear gradient of acetonitrile (0.1% TFA) over 50 min. Purified triN36e, obtained in 16% yield, was identified by ESI-TOF-MS. The detailed synthesis of peptides is described in the Supporting Information (SI).

CD Spectra. CD measurements were performed with a J-720 circular dichroism spectrolarimeter equipped with a thermoregulator (JASCO). The wavelength dependence of molar ellipticity [θ] was monitored at 25 °C from 190 to 250 nm. Peptides were dissolved in 20 mM acetate buffer (pH 4.0) containing 40% MeOH (*23, 24*). The experimental helicity was calculated as reported previously (*17*−*19*).

Immunization and Sample Collection. Six-week-old male BALB/c mice were purchased from Sankyo Laboratory Service Corp. (Tokyo, Japan) and maintained under specific pathogen-free conditions in an animal facility. The experimental protocol was approved by the ethical review committee of Tokyo Medical and Dental University. Freund incomplete adjuvant and PBS

* To whom correspondence should be addressed. E-mail: nomura.mr@tmd.ac.jp; tamamura.mr@tmd.ac.jp. phone: +81-3-5280-8036, fax: +81-3-5280-8039.

[†] Tokyo Medical and Dental University.

[‡] National Institute of Infectious Diseases.

10.1021/bc900502z
Published on Web 04/01/2010

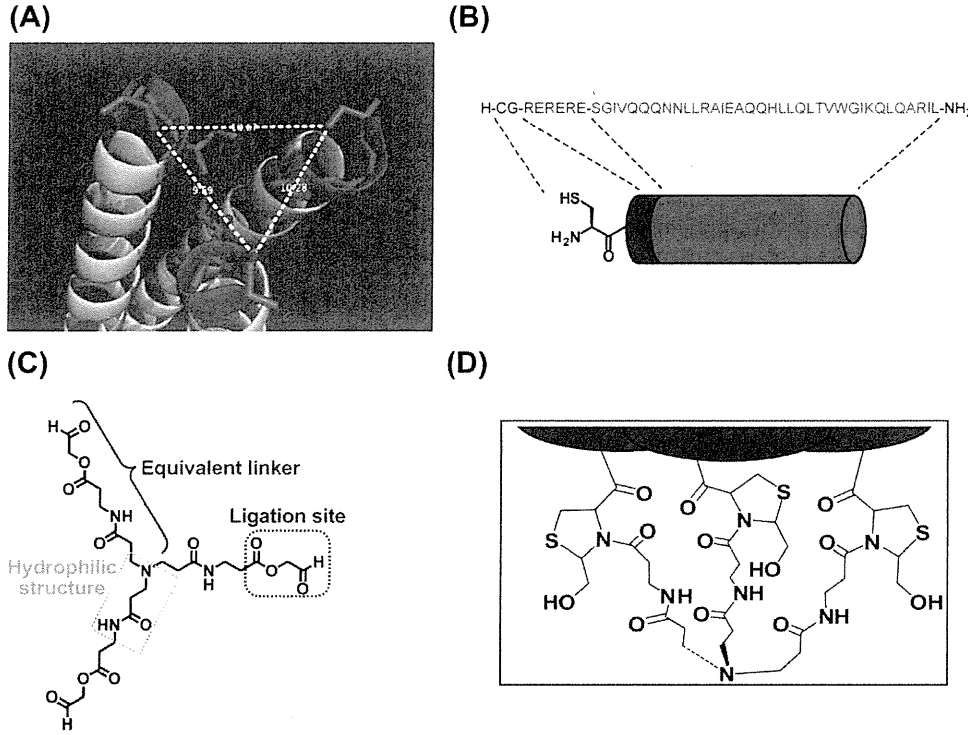

Figure 1. (A) Distances between hydrogen atoms for hydroxyl groups in N-terminal serine residues of N36 helices in trimeric form. The distances were evaluated by PyMOL (*21*). (B) Cartoon presentation of each N36 derived peptide, N36REGC. (C) Design of a C3-symmetric template. The amino acid residues are described in single letters. (D) Conjugated structure of trimeric N36 after thiazolidine ligation.

were purchased from Wako Pure Chemical Industries (Osaka, Japan). DMSO (endotoxin free) was purchased from Sigma-Aldrich (St. Louis, MO).

All mice were bled one week before immunization. One hundred micrograms of antigen was dissolved in 1 μL of DMSO. The solution was mixed with 50 μL of PBS and 50 μL of Freund incomplete adjuvant. The mixture was injected subcutaneously under anesthesia on days 0, 14, 28, 42, and 58. Mice were bled on days 21, 35, 49, and 65. Serum was separated by centrifugation (15 000 rpm) at 4 °C for 15 min and inactivated at 56 °C for 30 min. Sera were stored at −80 °C before use.

Serum Titer ELISA. Tween-20 (polyoxyethylene (20) sorbitan monolaurate) and hydrogen peroxide (30%) were purchased from Wako. ABTS (2,2-azino-bis(3-ethylbenzothiazoline-6-sulfonic acid) diammonium salt) was purchased from Sigma-Aldrich. Antimouse IgG (H+L)(goat)-HRP was purchased from EMD Chemicals (San Diego, CA). Ninty-six-well microplates were coated with 25 μL of a synthetic peptide at 10 μg/mL in PBS at 4 °C for overnight. The coated plates were washed 10 times with deionized water and blocked with 150 μL of blocking buffer (0.02% PBST, PBS with 0.02% Tween 20, containing 5% skim milk) at 37 °C for 1 h. The plates were washed with deionized water 10 times. Mice sera were diluted in 0.02% PBST with 1% skim milk, and 50 μL of 2-fold serial dilutions of sera from 1/200 to 1/102400 were added to the wells and allowed to incubate at 37 °C for 2 h. The plates were washed 10 times with deionized water. Twenty-five microliters of HRP-conjugated antimouse IgG, diluted 1:2000 in 0.02% PBST, was added to each well. After 45 min incubation, the plates were washed 10 times and 25 μL of HRP substrate, prepared by dissolving 10 mg ABTS to 200 μLof HRP staining buffer—a mixture of 0.5 M citrate buffer (pH 4.0, 1 mL), H_2O_2 (3 μL), and H_2O (8.8 mL)—was added. After 30 min incubation, the reaction was stopped by addition of 25 μL/well 0.5 M H_2SO_4, and optical densities were measured at 405 nm.

Virus Preparation. The pNL4-3 construct (8 μg) was transfected into 293T cells by Lipofectamine LTX (Invitrogen, Carlsbad, CA) followed by changing medium at 12 h after transfection. At 48 h after changing medium, the supernatant was collected, passed through a 0.45 μm filter, and stored at −80 °C as HIV-1_{NL4-3} strain before use. For titration, MT-4 cells were infected with serially 3-fold diluted virus from 1/10 to 1/196830, and cultured for 7 days. HIV-1 p24 levels in supernatants were measured, and then the titer of virus solution was calculated.

Anti-HIV Assay. Virus was prepared as described above except that the transfection of pNL4-3 was performed by the calcium phosphate method. Anti-HIV-1 activity was determined on the basis of protection against HIV-1-induced cytopathogenicity in MT-4 cells. Various concentrations of AZT, N36RE, and triN36e (The starting concentrations are 100, 10, and 1 μM, respectively) were added to HIV-1-infected MT-4 cells (MOI = 0.01) by 2-fold serial dilution and placed in wells of a flat-bottomed microtiter plate (2.0×10^4 cells/well). After 5 days' incubation at 37 °C in a CO_2 incubator, the number of viable cells was determined using the 3-(4,5-dimethylthiazol-2-yl)-2,5-diphenyltetrazolium bromide (MTT) method (EC_{50}). Cytotoxicity of compounds was determined on the basis of viability of mock-infected cells using the MTT method (CC_{50}). Each experiment was performed three times independently.

Neutralizing Assay. MT4-cells (1×10^5 cells/100 μL) were incubated in 100 μL medium containing 10 μL sera from immunized or preimmunized mice for 1 h at 37 °C, then pretreated MT-4 cells were infected with HIV-1_{NL4-3} (MOI = 0.05). At 3 days after infection, cells were collected by centrifuge at 4000 rpm for 10 min at 4 °C. After discarding supernatant, pellets were lysed with 30 μL of lysis buffer (50 mM Tris·HCl (pH 7.5), 150 mM NaCl, 1% NP-40), then 30 μL of 2 × SDS buffer (125 mM Tris·HCl (pH 6.8), 4% SDS, 20% glycerol, 10% 2-ME, 0.004% BPB) were added and boiled for 10 min. The samples (5 μL) were subjected to SDS-page to perform Western blotting. The HIV-1 gag p24 was detected by using Western lightning ECL kit (PerkinElmer, MA) according to manufacturer's instruction after treatment of HIV-1 p24

Scheme 1. Synthesis of the Equivalently Branched Template 6

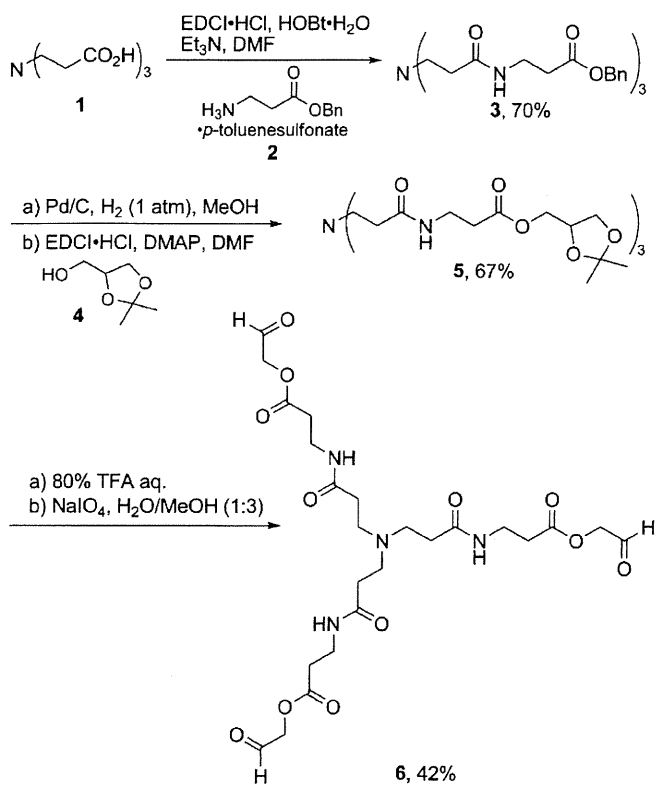

antibody (2C2; 1:2000 dilution) (*20*) and anti- mouse IgG (H+L)-HRP (Millipore, MA). The band intensity of p24 was calculated with post/pre-immunized samples by using *ImageJ* image analyzing software.

RESULTS AND DISCUSSION

The N-region of gp41 is known to be an aggregation site involving a trimeric coiled-coil conformation. In design of an N36-derived peptide (N36RE), the triplet repeat of arginine and glutamic acid was fused to the N-terminus to increase the solubility in buffer solution (Figure 1B). In order to form a triple helix corresponding precisely to the gp41 prefusion form, we designed the novel C3-symmetric template depicted in Figure 1C. This designed template linker has three branches of equal length and possesses the hydrophilic structure and ligation site for coupling with N36RE. The template was synthesized from the commercially available 3-[bis(2-carboxyethyl)amino]propanoic acid **1** as shown in Scheme 1. Coupling of **1** with β-alanine benzyl ester **2** gave the corresponding triamide **3** in 77% yield. Cleavage of three benzyl esters by hydrogenation and coupling with solketal **4** produced the corresponding triester **5**. Deprotection of the acetonides with aqueous 80% TFA followed by oxidative cleavage of diol group led to the desired template **6**. This approach uses thiazolidine ligation for chemoselective coupling of Cys-containing unprotected N36RE (N36REGC) with a three-armed aldehyde scaffold producing triN36e (Figure 1D). Thiazolidine ligation is a peptide segment coupling strategy which does not require side chain protecting groups (*22*−*26*). The reaction consists of three steps: (i) aldehyde introduction, in which a masked glycolaldehyde ester is linked to the carboxyl terminus of an unprotected peptide by reverse proteolysis; (ii) ring formation, in which the unmasked aldehyde reacts at acidic pH with the α-amino group of an N-terminal cysteine residue of the second unprotected peptide forming a thiazolidine ring; and (iii) rearrangement at higher pH in which O-acyl ester linkage is converted to an N-acyl amide linkage forming a peptide bond with a pseudoproline structure (Figure 2).

Circular dichroism (CD) spectra of triN36e and N36RE, which is a monomer form without N-terminal Cys-Gly residues, are shown in Figure 3A. The peptides were dissolved in 20 mM acetate buffer with 40% MeOH, pH4.0, suitable for measurement of CD spectra of membrane proteins (*27, 28*). Both spectra display double minima at 208 and 222 nm and showed high molar ellipticity as absolute values (Table 1). The results indicate that these peptides form a highly structured α-helix and that the helical content of the trimer triN36e is higher than that of the monomer N36RE. Furthermore, to assess the interaction of triN36e with C34, CD spectra of the peptide mixture with C34-derived peptide, C34RE, were measured (Figure 3B,C). The spectrum of triN36e and C34RE mixture showed high molecular ellipticity as an absolute value comparable with that of triN36e alone. This supports the conclusion that C34RE interacts with tri36e and thereby induces a higher helical form as shown previously (*29*).

Mice were immunized with these synthetic gp41 mimetics and antibody production was successfully induced (the detailed titer increase in 5 weeks' immunization is given in the Supporting Information). Two out of three mice showed induction of antibodies against either antigen (N36RE or triN36e). Antibody titers and selectivity of antisera isolated from mice immunized with N36RE or triN36e were evaluated by serum titer ELISA against coated synthetic antigens. The most active antiserum for each antigen was utilized for the evaluation of binding activity by ELISA (Figure 4). The N36RE-induced antibody showed approximately 5 times higher affinity for N36RE than for triN36e, as 50% bound serum dilutions are 3.88×10^{-4} and 2.14×10^{-3} to N36RE and triN36e, respectively. It is noteworthy that the triN36e-induced antibody showed approximately 30 times higher preference in binding affinity for triN36e antigen than for N36RE (serum dilutions at 50% bound are 3.83×10^{-3} to N36RE and 1.33×10^{-4} to triN36e). Although this evaluation was not determined with purified mAbs, it is clear that the antibodies produced exploit a structural preference for antigens. The mechanism of induction

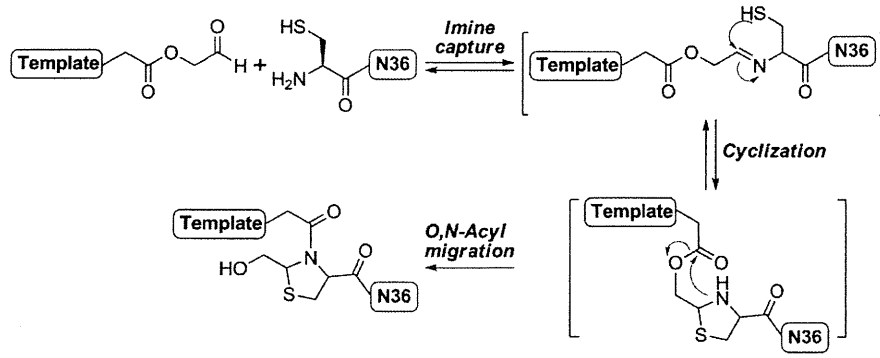

Figure 2. Reaction mechanisms of thiazolidine ligation utilized for assembly of N36RE helices on the template.